be expected that the $\frac{5}{2}^-$ and $\frac{7}{2}^-$ states in ^{63}Cu which apparently have quite different wave functions would also have different asymmetries. The fact that present measurements rule out large differences might be explained, however, on the basis that the single-particle contributions to these transitions are too small to affect the shape.)

Present indications are, then, that a more complex interaction is needed if the microscopic model is to work. While the addition of spin transfer did not affect the predictions very much, tensor interactions and the effects of antisymmetrization[54] should also be included in the calculations. Asymmetry data will provide a good test of such new calculations.

[54] K. A. Amos, V. A. Madsen, and I. E. McCarthy, Nucl. Phys. A94, 103 (1967).

ACKNOWLEDGMENTS

The authors gratefully acknowledge the indispensable help of R. Chaminade and the electronics group, Mrs. A. Garin and her co-workers in the detector laboratory, and of the entire cyclotron operating staff. A. Papineau kindly aided in several phases of the experimental work. We are indebted to Dr. J. Delaunay and Dr. P. Kossanyi-Demay for several calculations mentioned here, and to Dr. A. Forest for his microscopic-model form-factor program. We also thank Dr. M. Fricke, Dr. N. Glendenning, Dr. J. Lowe, Dr. F. G. Perey, Dr. G. R. Satchler, and Dr. A. Zucker for sending us unpublished reports of their work, as well as for several valuable discussions. The helpful comments of Dr. A. G. Blair, especially in the preparation of this paper, are greatly appreciated.

PHYSICAL REVIEW VOLUME 164, NUMBER 4 20 DECEMBER 1967

Study of Proton Particle-Hole States in ^{40}Ca by the ^{39}K(^{3}He,d)^{40}Ca Reaction*

KAMAL K. SETH
Northwestern University, Evanston, Illinois

AND

J. A. BIGGERSTAFF, P. D. MILLER, AND G. R. SATCHLER
Oak Ridge National Laboratory, Oak Ridge, Tennessee

(Received 7 July 1967)

Helium-3-induced charged-particle reactions on ^{39}K have been studied using a solid-state-detector dE/dx-E particle-identification telescope. Elastic-scattering angular distributions at ^{3}He energies of 12, 14, and 16 MeV as well as (^{3}He,d) angular distributions at 14 MeV have been measured. The reaction data are found to be characterized by extremely weak transitions to all known positive-parity excited states up to 5.3 MeV. Strong transitions to 15 negative-parity states up to 8.6-MeV excitation are observed and identified with the $T=0$ components of $(d_{3/2}^{-1}f_{7/2})$ and $(d_{3/2}^{-1}p_{3/2,1/2})$ configurations and the $T=1$ analogs of the ground-state quartet in ^{40}K having the $(d_{3/2}^{-1}f_{7/2})$ configuration. Since the distorted-wave method does not give a unique prescription for choosing between the various possible optical potentials which fit elastic scattering, a detailed examination is made of the effects of the choice specific ^{3}He and deuteron potentials, of the inclusion of spin-orbit coupling and nonlocality, and of the different approximations for the bound-state wave function; and the significance of the spectroscopic factors is discussed. The distorted-wave results are compared with the revised predictions of Gillet and Sanderson, and it is concluded that above and beyond the inherent uncertainties in the spectroscopic factors, Gillet and Sanderson's theoretical predictions agree poorly with the experimental results.

I. INTRODUCTION

IN the nuclear shell model ^{40}Ca, like ^{16}O, is of special importance because of its double-closed nature. In terms of the elementary shell model, the low-lying states of ^{40}Ca should have particularly simple particle configurations. The ground state should be doubly closed and spherical. The low-excitation negative-parity states should have 1-particle–1-hole configurations, with the particle being in the $f_{7/2}$, and $p_{3/2}$ (and to some extent $p_{1/2}$) orbitals and the hole being in the $d_{3/2}$ (and to some extent $s_{1/2}$ and $d_{5/2}$) orbitals. These negative-parity states should include two quartets of states with configurations $(d_{3/2}^{-1}f_{7/2})_{T=1}$ and $(d_{3/2}^{-1}p_{3/2})_{T=1}$. These are the analogs of the corresponding states[1] in ^{40}K and should start at approximately 7.6- and 9.6-MeV excitation, respectively, in ^{40}Ca. The positive-parity states are expected to be more complicated, involving excitations of $2p$-$2h$, $4p$-$4h$, etc., and having collective nature

* Research jointly sponsored by the U. S. Atomic Energy Commission under contract with Union Carbide Corporation and U. S. Army Research Office (Durham) under contract with Northwestern University.

[1] P. M. Endt and C. Van der Leun, Nucl. Phys. 34, (1962).

not unlike that found[2] in ^{16}O. In the simplest description of the negative-parity states, no appreciable T mixing or l (of the orbitals) mixing may be expected. However, recent random-phase-approximation (RPA) calculations by Gillet and Sanderson[3] (henceforth referred to as GS) predict that the ground state is doubly closed only about 35% of the time and very rarely are configurations for excited states pure in T or l. While for the negative-parity states no other detailed theoretical calculations exist,[4] the GS prediction for the ground state can be compared with that due to Gerace and Green.[5] These authors construct the even-parity states of ^{40}Ca as mixtures of double-closed $2s$-$1d$ shell-model states with two intrinsic deformed states formed by raising two and four particles from the $2s$-$1d$ shell to the $2p$-$1f$ shell. In contrast to GS they obtain the ground state as 82% doubly closed shell-model state. The amount of mixing predicted by GS for excited states is so much that one expects to be able to verify it experimentally and thus provide a good test of the RPA method or at least of the approximations and parameters used in the calculation of GS.

In this paper we report on the single-proton transfer reaction ^{39}K(^{3}He,d)^{40}Ca. To the extent that the ground state of ^{39}K can be described as a pure $d_{3/2}$ proton hole, and the stripping reaction mechanism is not expected to excite the core appreciably, the states reached by this reaction should be those with parentage in the $d_{3/2}$ proton hole. States which have the proton hole in the $s_{1/2}$ or $d_{5/2}$ orbitals, or states which involve neutron excitations, are expected to have poor overlap with the ^{39}K ground-state wave function and transitions to them and to the positive-parity states should be strongly inhibited. As far as the analysis of the observed angular distribution is concerned, the distorted-wave theory of (^{3}He,d) stripping should be ideally suited for analyzing the angular distributions observed in this reaction because of the expected single-particle ($+^{39}$K core) nature of the states in question. The observed angular distributions may therefore be used to test the distorted-wave theory, or rather the practical aspects of its application. Indeed, we devote a substantial part of this paper to just such investigations. We discuss the sensitivity of the predicted angular distributions and the deduced spectroscopic factors to the parameters of the optical potentials, to the nonlocality of the potentials, to the inclusions of spin-orbit potential, and to prescription for the calculation of the bound states.

An investigation of the same reaction has recently been made by Erskine[6] at 12 MeV, and we also present a comparison of our results with his and show that the differences are largely accounted for by differences in the distorted-wave analysis.

II. EXPERIMENTAL METHOD

The experiments reported here were done using ^{3}He beams of energies between 12 and 16 MeV, obtained from the Oak Ridge National Laboratory EN tandem accelerator. The duo-plasmatron source provided approximately 60 na of ^{3}He beam on the target through two beam defining slits, 22 in. apart, and each of dimensions $\frac{1}{16}\times\frac{3}{16}$ in.

A. Targets

In the experiments reported here, approximately 100 μg/cm^2 natural potassium targets evaporated on 30 μg/cm^2 carbon backings were employed. Both carbon and gold were investigated as backing materials. In magnetic spectrographs momentum selection and use of absorber foils in front of photographic plates permit one to avoid the problems associated with excessive elastic-scattering yield at forward angles without any loss of energy resolution. However, in order to preserve good energy resolution, absorber foils cannot be used with solid-state detectors and all reaction products have to be handled by the associated electronic circuitry. For this reason, in spite of the fact that gold has the advantage of having a large Coulomb barrier and, therefore, much smaller yield for its reaction groups, carbon was preferred as backing material because it permitted data to be taken at more forward angles. For the same reason KI and KBr were ruled out as target materials and metallic potassium targets were used.

Because of the highly reactive nature of potassium, target evaporation had to be done essentially in the scattering chamber. This was achieved by attaching a small evaporator assembly at the bottom of the chamber. This assembly could be separately pumped and could be isolated from the chamber by a gate valve during loading, unloading, and outgassing of potassium. The target was designed so that when a target blank with carbon backing was lowered through the open gate valve in position for evaporation, a part of the target ladder sealed the scattering chamber from the evaporator. This feature prevented the chamber and the detectors from being exposed to the potassium vapors during evaporation. The success of our evaporation technique is illustrated by the fact that (judging from the relative yields of the deuteron groups to the 7.53-MeV level in ^{40}Ca and the ground state of ^{17}F) our oxygen contamination using metallic potassium was about 30% less than that realized by Erskine with KI target. The 7% abundance of ^{41}K in natural potassium did not, in general, present much of a problem, although deuteron groups to several low-lying states in ^{42}Ca could be clearly identified.

[2] E. B. Carter, G. E. Mitchell, and R. H. Davis, Phys. Rev. **133**, B1421 (1964).
[3] V. Gillet and E. A. Sanderson, Nucl. Phys. **54**, 472 (1964); **A91**, 292 (1967). The latter is referred in this article as GS.
[4] H. Horie and T. Yokazawa, Phys. Letters **7**, 145 (1963).
[5] W. J. Gerace and A. M. Green, Nucl. Phys. **A93**, 110 (1967).
[6] J. R. Erskine, Phys. Rev. **149**, 854 (1966).

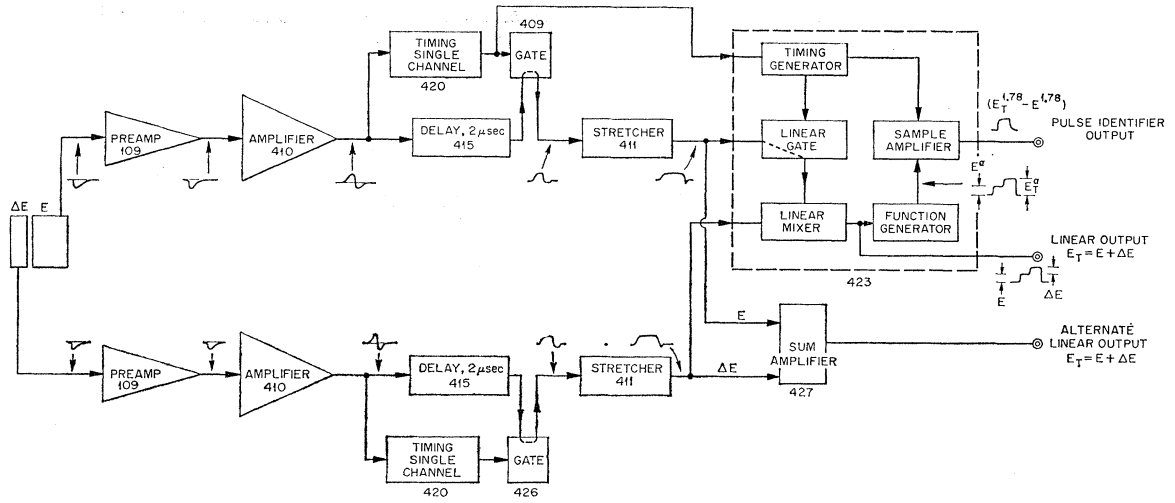

FIG. 1. Schematic diagram of particle detection and identification circuitry.

B. Particle Detection and Identification

This experiment was done in conjunction with our investigation[7] of the $^{39}K(^3He,p)^{41}Ca$ and $^{39}K(^3He,\alpha)^{38}K$ reactions. Since protons of energies up to 23 MeV were expected for an incident ^3He energy of 14 MeV, silicon detectors of total depletion depth of about 3.2 mm were required and particle identification was considered necessary. A dE/dx-E telescope, consisting of a 260-μ totally depleted silicon surface-barrier detector was used as the ΔE detector and a 3-mm Li-drifted silicon detector was used as the E detector. The E lithium-drift detector was cooled by circulating trichloroethylene, chilled to dry-ice temperature, through a jacket surrounding the detector.

Our choice of the ΔE detector thickness and the particle identification scheme was determined by the following considerations. The commonly used methods of electronic particle identification are based on the differential energy-loss relation

$$(dE/dx)\simeq C_1(mz^2/E)\ln(C_2m/E), \quad (1)$$

where C_1 and C_2 are constants for the given stopping material, and m and z are the mass and charge of the incident particle. Equation (1) suggests that particle identification can be done by the use of a two-detector telescope, the first (ΔE) detector being relatively thin in order to measure partial energy loss, and the second (E) detector being thick enough to completely stop particles of the residual energy $E=E_t-\Delta E$. Such a telescope can be used in two ways. If the ΔE detector is very thin, Eq. (1) gives $E_t\times\Delta E$ approximately proportional to mz^2. For moderate thickness detectors the relation which has been empirically determined to be satisfactory is

$$(E+a\Delta E+b)\Delta E\propto mz^2, \quad (2)$$

where a and b are constants for a given ΔE detector. For thicker ΔE detectors upon integration, Eq. (1) yields $[(E+\Delta E)^2-E^2]$ approximately proportional to mz^2. The more accurate empirical relation is

$$[(E+\Delta E)^\alpha-E^\alpha]\propto mz^2. \quad (3)$$

In agreement with Goulding[8] we have found $\alpha=1.75\pm0.02$ suitable for energies between 5 and 25 MeV for ΔE detector thicknesses between 50 and 500 μ.

In this experiment, we did not wish to identify ^3He from ^4He, but rather to achieve the best resolution possible. For this reason, we elected to use a thick ΔE detector. Such detectors are more uniform, have less capacitance, and provide better energy resolution than the thin ones. We chose a 260-μ surface-barrier silicon detector for this purpose since it would completely stop

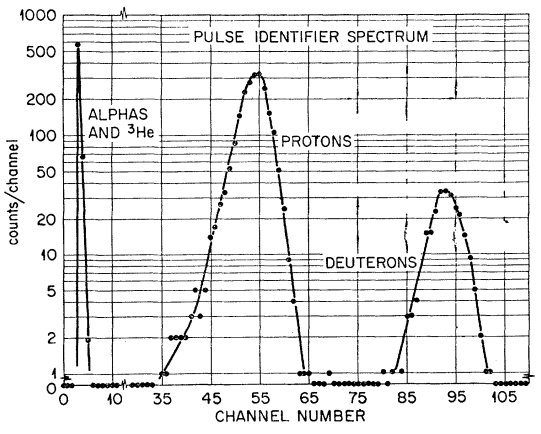

FIG. 2. Particle identifier output. This output was used to set digital discriminators to route α, p, and d spectra to three separate quarters of the 4096-channel analyzer.

[7] K. K. Seth, J. A. Biggerstaff, and P. D. Miller, Phys. Rev. Letters **17**, 1294 (1966).

[8] F. S. Goulding, D. A. Landis, J. Cerny III, and R. H. Pehl, Nucl. Instr. Methods **31**, 1 (1964).

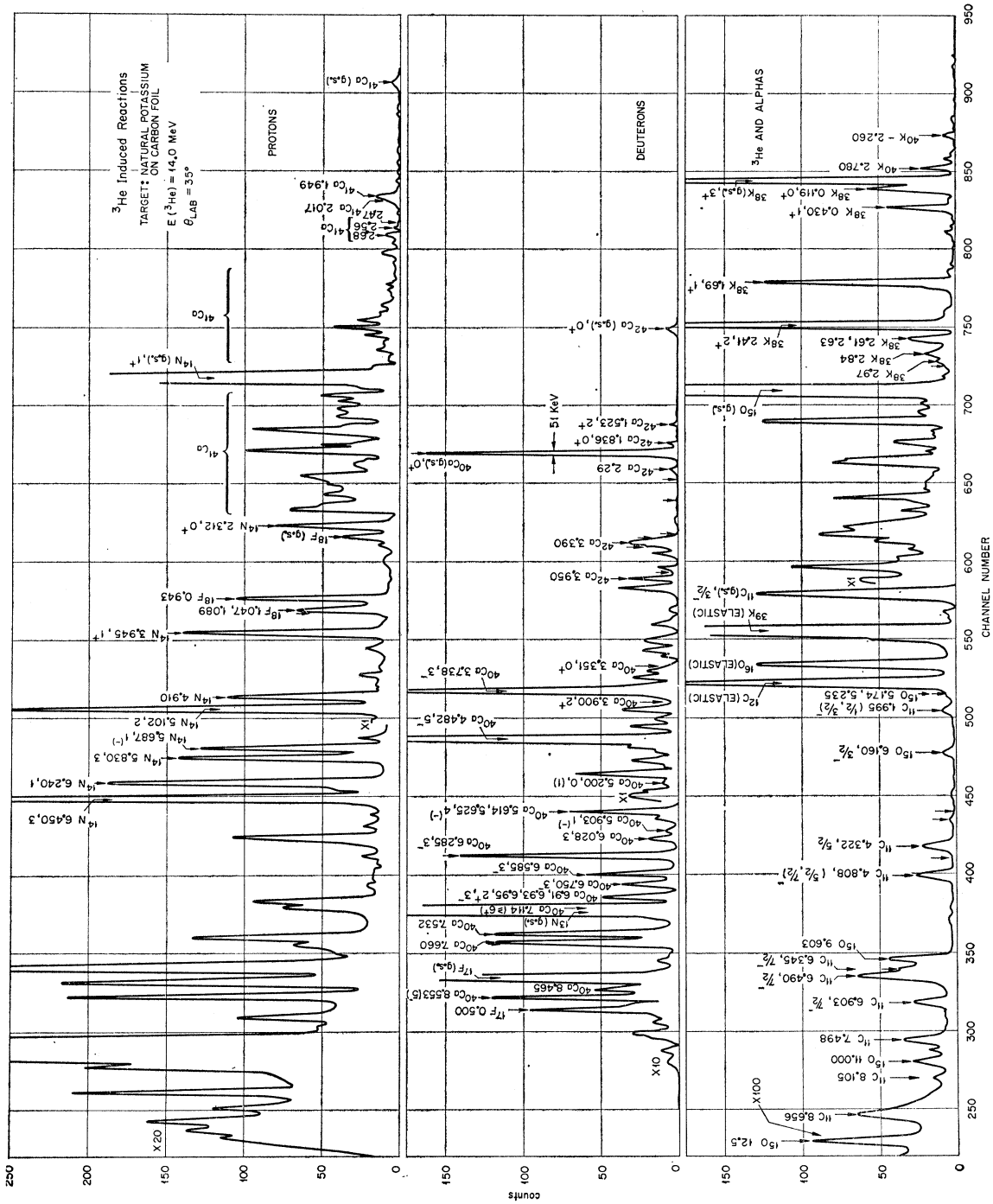

FIG. 3. Typical particle-identified spectrum.

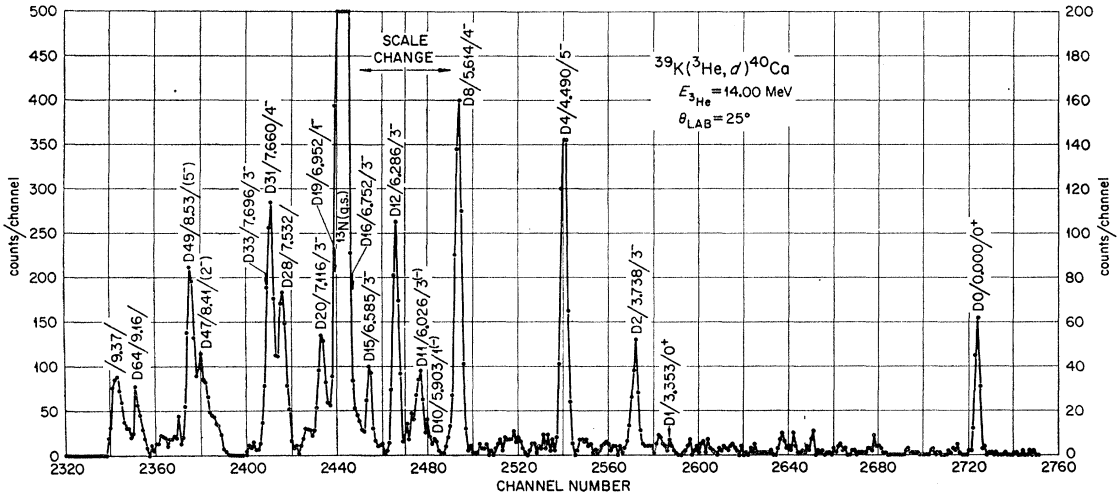

FIG. 4. Details of reduced deuteron spectrum at $\theta_{lab}=25°$. Notice that at this angle the ^{13}N(g.s.) peak obscures the 6.75- and 6.95-MeV ^{40}Ca groups.

the highest-energy (21.5 MeV) α particles expected and the entire α spectrum could be preserved and identified by anticoincidence with pulses from the follow-up E detector. In order to obtain the function on the left-hand side of Eq. (3) from the observed quantities E and ΔE, we used the circuitry shown in Fig. 1, which includes an ORTEC prototype of the Goulding-type particle identifier. The use of the identifier at energies above 10 MeV has been described in detail by Goulding.[8] In our use we made the following modifications in order to preserve the α-particle spectrum which would be lost in Goulding's original manner of use of the circuit. We did not require coincidence between ΔE and E signals. Instead, we used the crossover signal from the timing single-channel analyzer for the E channel as both the coincidence and timing signals for the particle identifier. Further, in order to preserve the α spectrum and in the interest of best resolution and linearity, we summed the ΔE and E signals outside of the particle identifier. In summing the E and ΔE signal, compensation was made for the incomplete charge collection in the thick E lithium-drift detector. The sum signal was analyzed by the 1024-channel analog-to-digital convertor (ADC) of a Nuclear Data 4096-channel analyzer.

Figure 2 illustrates the particle identifier output (PIO). It is obvious that particle separation is very good. The particle identifier output was used through digital discriminators to route the E signal into three separate quadrants of 1024 channels each:

1st quadrant: no PIO output, all ^3He and ^4He particles, protons below 5.5 MeV and deuterons below 7.3-MeV energy;

2nd quadrant: all protons above 5.5 MeV;

3rd quadrant: all deuterons above 7.3 MeV.

The quality of the particle identification is also illustrated by Fig. 3, where identified particle spectra are shown for the ^3He-induced reactions at 35°. The deuteron groups from states at 7.66 and 7.53 are clearly separated from the proton group from a state which falls exactly between the two deuteron energies. The over-all energy resolution obtained was 40 keV for protons and 50 keV for deuterons. This is good, since individual detector resolutions were approximately 20 keV for ΔE detector and 25 keV for E detector. Kinematic energy spread and finite target thickness account for the rest.

The analyzer was calibrated with a precision charge pulser[9] and the calibration was checked against the energies of the well-known groups in ^{13}N and ^{14}N. The Q values (based on experimental results and known masses) used for this purpose were

$$^{12}C(^3He,p)^{14}N: \quad Q_0=4.7786\pm0.0003 \text{ MeV},$$
$$^{12}C(^3He,d)^{13}N: \quad Q_0=-3.5498\pm0.0011 \text{ MeV}.$$

The observed energy spectra for deuterons were analyzed manually after subtracting a smooth background. An example of the reduced deuteron spectrum is shown in Fig. 4.

III. EXPERIMENTAL RESULTS

A. Elastic Scattering

Measured elastic-scattering angular distributions, plotted as $(d\sigma/d\sigma_{Ruth})$ versus $\theta_{c.m.}$ for incident ^3He energies of 12, 14, and 16 MeV, are shown in Figs. 5 and 6, along with optical-model fits to the data. A single absolute normalization was determined by the optical-model fits to the elastic-scattering data and all three elastic scattering and the 15 $(^3He,d)$ angular distributions were normalized to it. The fits are discussed in Sec. IV.

[9] J. A. Biggerstaff (unpublished). The pulser has a linearity of better than 10 ppm.

TABLE I. Q values and excitation energies in ^{40}Ca.

	Present experiment ^{39}K(^{3}He,d)^{40}Ca		Erskine ^{39}K(^{3}He,d)^{40}Ca	Grace and Poletti ^{40}Ca(p,p')^{40}Ca
	Q[a]	E^*[b]	E^*[b]	E^*[b]
Dn	MeV (±keV)	MeV (±keV)	MeV (±keV)	MeV (±keV)
$D0$	2.845 (8)	0	0	0
$D2$	−0.889 (10)	3.734 (6)	3.738 (5)	3.731 (10)
$D4$	−1.641 (10)	4.486 (6)	4.490 (5)	4.482 (10)
$D8$	−2.776 (12)	5.621 (9)	5.614 (6)	5.619 (10)
$D10$	...[c]	...[c]	5.902 (6)	5.903 (10)
$D11$	...[c]	...[c]	6.026 (5)	6.028 (10)
$D12$	−3.449 (12)	6.294 (9)	6.286 (5)	6.285 (10)
$D15$	−3.741 (10)	6.586 (6)	6.585 (6)	6.583 (10)
$D16$	−3.905 (10)	6.750 (6)	6.752 (6)	6.750 (10)
$D19$	−4.107 (10)	6.952 (6)	6.952 (6)	6.948 (10)
$D20$	−4.273 (10)	7.118 (6)	7.116 (6)	7.114 (10)
$D28$	−4.691 (12)	7.536 (9)	7.532 (6)	7.531 (10)
$D31$	−4.829 (15)	7.674 (13)	7.660 (6)	7.655 (10)
$D33$			7.696 (6)	7.696 (10)
$D47$	−5.590 (12)	8.435 (9)	8.465 (12)	8.424 (10)
$D49$	−5.710 (12)	8.555 (9)	8.553 (9)	8.535 (10)

[a] The errors in Q values quoted in parentheses included estimate of calibration error (±8 keV) and the error $\pm 2\sigma$, where σ is the standard deviation of the observed values for the ten angles between 25° and 70°.
[b] *Absolute* errors (in keV) are indicated in parentheses. In all cases errors in energy *differences* are approximately half of these.
[c] Counting statistics for these groups were too low to permit an accurate determination of energies.

B. (^{3}He,d) Reaction

The exact peak location for the deuteron groups was determined by Lagrangian interpolation to a given line shape and Q values corresponding to the peaks were obtained by using relativistic kinematics with the energy calibration described before. The effects of target and backing thicknesses, target orientation, and angle of observation were taken into account. Q values so determined for the ground-state and 15 excited states were found to be consistent for the ten angles of observation from 20° to 70°. The quantity 2σ, where σ is the standard deviation, was generally less than 6 keV. These Q values, and the corresponding excitation energies, are listed in Table I, along with energies determined in the ($p,p'\gamma$) experiments of Grace and Poletti,[10] and the (^{3}He,d) experiments of Erskine,[6] both using magnetic spectrographs. The states in ^{40}Ca are labeled according to the sequence given by Grace and Poletti. We find $Q_0 = 2.845 \pm 0.008$ MeV. This is in excellent agreement with the value 2.840 ± 0.004 MeV, determined from masses. Our excitation energies are similarly in very good agreement with both magnetic spectrograph results. The agreement with Erskine is poor only for the state at 8.435 MeV for which the discrepancy is as much as 30 keV. This is perhaps explainable. In this energy region, Erskine observed several contaminant groups and states that these groups "may have been misidentified." For all other states throughout this paper we adopt Erskine's energies.

The most significant observation about the deuteron groups concerns the groups not seen. The reaction is obviously highly selective as anticipated in the introduction. The well-known positive-parity excited states[1] at 3.353 (0^+), 3.900 (2^+), 5.200 ($0^{(+)}$), 5.244 ($2^{(+)}$), and 5.274 ($4^{(+)}$) are barely observed and upper limits on

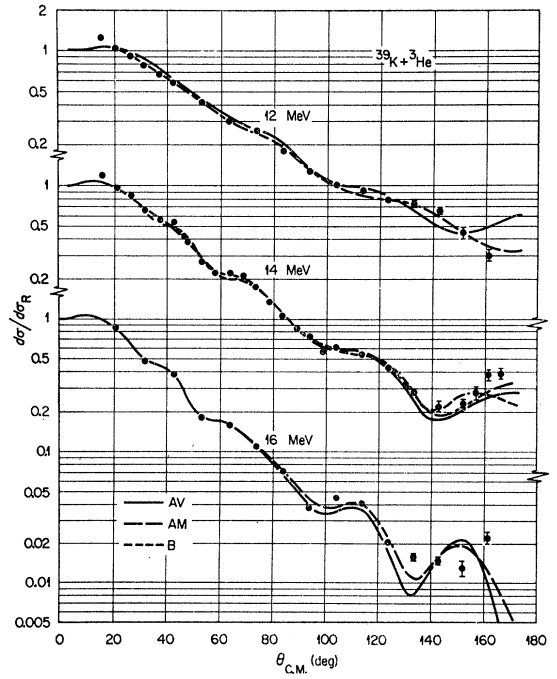

FIG. 5. Optical-model fits to the elastic-scattering data with potentials described in Table II and the text. No spin-orbit coupling was included in these potentials.

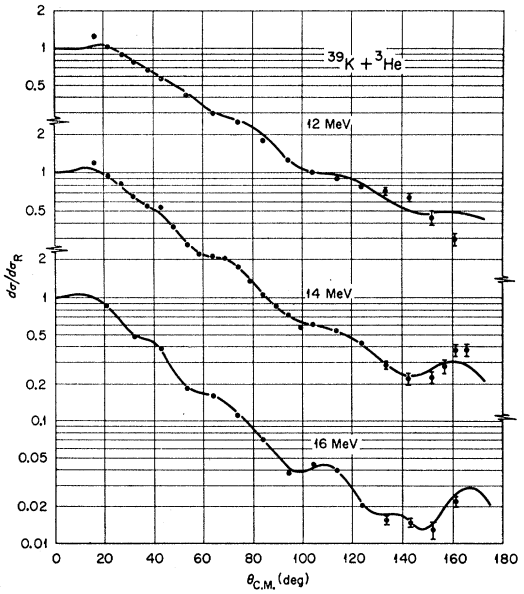

FIG. 6. Optical-model fits to the elastic-scattering data with potentials including spin-orbit term as described in Table II and the text.

[10] M. A. Grace and A. R. Poletti, Nucl. Phys. **78**, 273 (1966).

their strength referred to the ground state can be placed as following: 3.353 ($\leq 8\%$), 3.900 ($\leq 3\%$), and 5.200 +5.244+5.274 ($\leq 10\%$). We shall have occasion to refer to the state at 3.353 MeV later in Sec. VI.

IV. ANALYSIS OF ANGULAR-DISTRIBUTION DATA

A. Optical-Model Analysis of Elastic Scattering

The elastic scattering was analyzed using an optical-model potential of the usual form:

$$U(r)=-V(e^x+1)^{-1}-i(W-4W_D d/dx')(e^{x'}+1)^{-1}, \quad (4)$$

where

$$x=(r-r_0A^{1/3})/a, \quad x'=(r-r_0'A^{1/3})/a',$$

together with the Coulomb potential from a uniformly charged sphere of radius $r_cA^{1/3}$, with $r_c=1.4$ F. Following previous work,[11–15] only volume absorption was used ($W_D=0$). Spin-orbit coupling was not included in most of this work because the elastic scattering at these energies is known to be fairly insensitive to it. The optimum values of the parameters were obtained by using the automatic search routine[16] "Hunter." This minimizes the quantity

$$\chi^2=N^{-1}\sum_{i=1}^{N}[\sigma_{\mathrm{Ex}}(\theta_i)-\sigma_{\mathrm{Th}}(\theta_i)]^2/\Delta\sigma_{\mathrm{Ex}}(\theta_i)^2,$$

where σ_{Ex} and σ_{Th} are the measured and predicted cross sections, respectively, while $\Delta\sigma_{\mathrm{Ex}}$ is the error associated with σ_{Ex}.

1. Ambiguities

There are considerable ambiguities in the determination of optical parameters for strongly absorbed particles, of both the continuous and the discrete type.[17] The former are associated with small, correlated variations in two or more parameters, which leave the scattering approximately unchanged. The latter give rise to a series of families of potentials which differ from one another, roughly, by the number of half-wave lengths enclosed in the nuclear interior. We shall concentrate our attention on two of these families which have been used successfully in other analyses of (^{3}He,d) reactions.[6,14,18] They also satisfy the suggested requirement that the real part of the optical potential for a mass-3 particle should be approximately three times that for a sincle nucleon. Unfortunately this requirement is not unambiguous. If the ^{3}He potential were to be obtained by averaging the real parts of the potentials for its constituent nucleons over their motion in the ^{3}He, the resulting potential[19] would have a radius close to that for the nucleons ($r_0\approx 1.25$ F, say), a larger surface diffuseness ($a\approx 0.7$ F, say) and a depth of about 150 MeV. A potential of this type, with $r_0=1.244$ F, $a=0.686$ F, and $V\approx 150$ MeV, has been found by Bassel[12] to give a good description of 22-MeV ^{3}He scattering from a large range of nuclei, but with masses greater than the ^{39}K considered here. Here we call this potential type B. The imaginary part of this potential is found to have a larger radius than the real part.

However, when one searches for optimum values of r_0 and a using the χ^2 criterion, there is a definite tendency for the radius to be smaller, and the diffuseness larger, than in the type-B potential. Judged subjectively, the improvement in fit obtained is often very small, so it is difficult to know how physically significant is this tendency, even though it appears systematically. A similar trend is observed in the analysis of deuteron scattering. When this occurs, it is not clear how to apply the criterion that the potential should be approximately three times that for a nucleon. If we stay within the family which includes the type-B potential, the decreasing radius is accompanied by an increasing depth; in the present case we shall see we are led to potentials which we shall call type D, in which $r_0\approx 200$ MeV. If, however, even with the smaller radius, we prefer to keep the potential depth in the nuclear interior at the value $V\approx 150$ MeV, which is three times the depth for a single nucleon, we must transfer our attention to the adjacent, more shallow, family of potentials. In particular we have studied potentials with $r_0\approx 1.0$ F and $V\approx 160$ MeV which we call here type A.

Finally, we also investigate another choice, namely a potential within the family which contains type B, which has been found[13] to give a reasonable fit to the scattering of ^{3}He from ^{40}Ca at energies of 22, 37.7, and 64.3 MeV, as well as from a number of other nuclei. This has $r_0=1.14$ F, $a=0.723$ F, and the correspondingly larger $V\approx 180$ MeV; we call this type C.

2. Absolute Normalization

The absolute normalization of the cross sections considered was not known exactly, but was determined by two criteria. One was the quality of fit obtained with the optical-model potentials both when *all* the parameters were varied to minimize χ^2 and when r_0 and a were constrained to have the values of the type-B and type-C potentials just described. The normalizations arrived at agreed to within a few percent. The other criterion,

[11] J. L. Yntema, B. Zeidman, and R. H. Bassel, Phys. Letters **11**, 302 (1964).
[12] D. D. Armstrong, A. G. Blair, and R. H. Bassel (to be published).
[13] E. F. Gibson, B. W. Ridley, J. J. Kraushaar, M. E. Rickey, and R. H. Bassel, Bull. Am. Phys. Soc. **11**, 118 (1965); Phys. Rev. **155**, 1194 (1967).
[14] J. C. Hiebert, E. Newman, and R. H. Bassel, Phys. Rev. **154**, 898 (1967).
[15] D. Cline, W. R. Alford, and L. M. Blau, Nucl. Phys. **73**, 33 (1965).
[16] R. M. Drisko (unpublished).
[17] R. M. Drisko, G. R. Satchler, and R. H. Bassel, Phys. Letters **5**, 347 (1963).
[18] R. H. Bassel, Phys. Rev. **149**, 791 (1966).
[19] J. R. Rook, Nucl. Phys. **61**, 219 (1965); A. Y. Abul-Magd and M. El-Nadi, Progr. Theoret. Phys. (Kyoto) **35**, 798 (1966).

TABLE II. Optimum optical-potential parameters for $^{39}K+^{3}He$.

Type	E (MeV)	V (MeV)	r_0 (F)	a (F)	M (MeV)	r_0' (F)	a' (F)	σ_A (mb)	χ^2
				Without spin orbit					
A	14	161.6	*1.0*[a]	*0.8*	13.1	1.622	0.780	1034	2.7
AM	14	169.4	0.961	0.829	12.7	1.657	0.740	1023	2.4
AM+	14	172.7	0.953	0.811	13.2	1.623	0.756	1003	3.4
AM−	14	173.4	0.937	0.859	12.2	1.694	0.725	1046	1.9
B	14	158.3	*1.244*	*0.686*	19.0	1.523	0.655	984	3.6
C	14	180.7	*1.14*	*0.723*	17.9	1.528	0.714	998	2.8
D	14	215.1	1.008	0.773	16.2	1.575	0.739	1017	2.5
A	12	148.9	*1.0*	*0.8*	11.3	1.759	0.882	1086	2.8
AM	12	268.8	0.617	0.962	8.9	1.880	0.771	1036	1.2
A	16	162.2	*1.0*	*0.8*	14.1	1.615	0.743	1099	10
AM	16	184.0	0.902	0.847	12.6	1.684	0.751	1144	9
AV	···	*162.0*	*1.0*	*0.8*	*13.0*	*1.62*	*0.8*	···	···
				With spin orbit; $V_s=7$ MeV					
AS	14	160.6	*1.0*	*0.8*	8.2	1.801	0.792	1102	2.0
AMS	14	198.7	0.852	0.847	7.7	1.837	0.780	1100	1.7
AS	16	160.3	*1.0*	*0.8*	8.6	1.778	0.779	1176	1.5
AMS	16	158.1	1.010	0.799	8.7	1.775	0.776	1175	1.5

[a] The italicized numbers were kept fixed during the search. The potentials AM+, AM− were obtained by fitting the 14-MeV data renormalized by ±5%, respectively.

which gave essentially the same results, was the cross section measured at 20° in the laboratory system. Although this is not equal to the Rutherford cross section, it is close to it and it was found that the value predicted by the optical model was fairly insensitive to the potential parameters. For example all the values for 14 MeV (over 100) encountered in the present studies fell in the range $d\sigma/d\sigma_R=0.94\pm0.03$. The values for $d\sigma/d\sigma_R$ at this angle finally adopted were 1.02, 0.96, and 0.86, at 12, 14, and 16 MeV, respectively, and the data were normalized accordingly. It is difficult to assess the probable error to be associated with a normalization obtained in this way, but it is probably not more than a few percent.

3. *Results*

Some results of these analyses are given in Table II. Greatest attention was given the 14-MeV data, both because they are the most extensive and because this is the energy used for the (^{3}He,d) measurements. The potentials called type A were obtained keeping fixed $r_0=1.0$ F and $a=0.8$ F. Searching for values of r_0 and a which minimized χ^2 then led to type AM. The types B, C, and D are members of the next deeper family of potentials, as just discussed. Figure 5 compares the data with some of the optical-model predictions. The solid curves were computed using the average parameters (called AV in Table II) based on the type-A fits. The over-all agreement is very good except at the largest angles. The angular distributions are very structureless, being dominated by the Coulomb and strong-absorption aspects of the interaction. It is only at the largest angles that a further variation in parameters, expecially in r_0 and a, produces any appreciable change. The predictions of the optimum AM potentials are shown as the curves with long dashes; the changes are slight. Also shown for 14 MeV is the curve with short dashes resulting from the type-B potential with its larger radius for the real potential. The oscillations in the angular distribution are now in slightly poorer agreement with the data, but the loss of quality is marginal. None of these studies succeeded in reproducing the 16-MeV distribution past 120°. The dip in the 12-MeV distribution beyond 140° is fitted by the AM potential, but only at the expense of a very small radius and a large diffuseness.

Also included in Table II are the type-A results at 14 MeV when other normalizations of the data were used. Potentials AM± correspond to normalizations differing by ±5% from that finally adopted, and the changes induced are not great. (It might be objected that χ^2 has a lower value for AM− than for AM; however, as was discussed above, the normalization adopted corresponding to AM was not chosen on this basis alone.

4. *Spin-Orbit Coupling*

It may be that little significance should be attached to the large-angle discrepancies. However, for completeness it was decided to see if including a spin-orbit coupling of the form

$$V_s(\hbar/m_\pi c)^2 r^{-1}(d/dr)(e^x+1)^{-1}\mathbf{L}\cdot\boldsymbol{\sigma}$$

would remove them. The value of V_s was not allowed to vary during the fitting procedure, but was fixed at $V_s=7$ MeV. Only the type-A potential was studied, and the results are also given in Table II. The predictions for the AS potentials are compared to the data in Fig. 6; the potential obtained for the 14-MeV data was also used at 12 MeV. There is a considerable improvement at 16 MeV for $\theta>100°$, with χ^2 reduced by a factor of 6. The improvement at 14 MeV is much less, and at 12 MeV is almost negligible. The main change in the

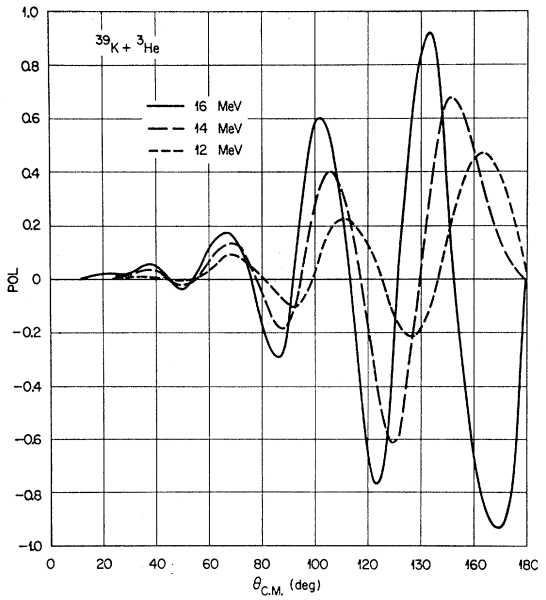

FIG. 7. Predicted polarization for elastic scattering of 12-, 14-, and 16-MeV ^{3}He from ^{39}K. The same potential was used for these calculations as for Fig. 6.

potentials is an increase of the imaginary radius to $r_0 \approx 1.8$ F, and a corresponding decrease in W.

Although the fit for large angles at 16 MeV is dramatically better, it is difficult to know whether this is not, in part, fortuitous. It will be necessary to have polarization data before the spin-orbit coupling is well determined. The polarizations corresponding to the cross sections of Fig. 6 are shown in Fig. 7. As has been discussed before,[12] the polarization is small in the forward hemisphere, and does not reach large values until the cross section is small. There is also a marked energy dependence in this energy region which may be attributed to the effects of the Coulomb barrier.

B. Distorted-Wave Analysis of Reaction Data

The distorted-wave theory of transfer reactions has been discussed in many places. In particular its application to (^{3}He,d) reactions (or their inverses) was studied in detail,[14,18] with the conclusion that it was a reliable tool for extracting both relative and absolute spectroscopic information from these reactions. It was used in the analysis of the earlier data on the ^{39}K(^{3}He,d) reaction.[6]

1. *Spectroscopic Factors*

The differential cross section for a target of spin J_0 can be written in the form

$$\frac{d\sigma}{d\omega}=\sum_{lj} G_{lj}\sigma_{lj}(\theta) \text{ mb/sr}, \quad (5)$$

where J is the spin of the residual nuclear state and G_{lj} is the partial strength for that state[20] for capture into the l, j orbit. Then $\sigma_{lj}(\theta)$ may be called the "single-particle" cross section for the transition; it is computed here with the normalization of approximation (b) of Bassel.[18] If the nuclear states have unique value of isospin, the partial strength G_{lj} may be factored as

$$G_{lj}=[(2J+1)/(2J_0+1)]C^2S_{lj}, \quad (6)$$

where S_{lj} is the conventional spectroscopic factor,[20] and C is the Clebsch-Gordan coefficient expressing conservation of the isospin,

$$C=\langle T_0, \tfrac{1}{2}, T_{03}, -\tfrac{1}{2} | T, T_{03}-\tfrac{1}{2}\rangle.$$

We assume $T_0=T_{03}=\frac{1}{2}$ for ^{39}K; then we may have $T=0$ or 1 for ^{40}Ca. For either choice, $C^2=\frac{1}{2}$, which merely expresses equal probabilities that an excited nucleon in the final state may be a neutron or a proton. If, however, the Coulomb interactions introduce isospin mixtures in the wave function of the final state, these contribute coherently to the nuclear overlap which defines the spectroscopic amplitude. We then have, in the notation of Ref. 20,

$$G_{lj}=[(2J+1)/(2J_0+1)]n[\sum_T C(T)g_{lj}(T)]^2. \quad (7)$$

For the (^{3}He,d) reaction this becomes[21]

$$G_{lj}=[(2J+1)/(2J_0+1)](n/2)[g_{lj}(T=0)+g_{lj}(T=1)]^2.$$

Nonetheless, since *in this particular case* $C=1/\sqrt{2}$ for both $T=0$ and $T=1$, we may use the quantity

$$S_l=2(2J_0+1)\sum_j G_{lj}/(2J+1)$$
$$=\sum_j |g_{lj}(T=0)+g_{lj}(T=1)|^2, \quad (8)$$

which becomes the usual spectroscopic factor, $S_l=\sum_j S_{lj}$, in the absence of T mixing. Mixing of $T=0$ and $T=1$ will allow $S>1$ (but always $S\leq 2$), representing a probability of greater than 50% that the nucleon excited is a proton.

When there is a unique T value, the spectroscopic factor is just $S_{lj}(T)=ng_{lj}^2(T)$. If, as here, the target consists of a hole in a closed shell and that hole is filled to form the ground state of the residual nucleus, we have $J=0$ and the angular momentum transferred is $j=J_0$. Further,

$$g_{lj}(T)=\delta_{T,0}\delta_{j,J0},$$

and the number of nucleons in the shell is $n=2(2J_0+1)$. Hence $G=1$ for this transition. When the residual state is regarded as a mixture of particle-hole configurations, $n=1$ and the g_{lj} are the amplitudes for the components of the wave function in which the hole state is the

[20] M. H. Macfarlane and J. B. French, Rev. Mod. Phys. **32**, 567 (1960); J. B. French and M. H. Macfarlane, Nucl. Phys. **26**, 168 (1961).

[21] The *difference* between the $T=0$ and 1 amplitudes would appear for the analogous ^{39}Ca(t,d) reaction.

TABLE III. Deuteron optical potentials used in the distorted-wave calculations.

Type	V (MeV)	r_0 (F)	a (F)	W_D (MeV)	r_0' (F)	a' (F)
Z	112	1.0	0.90	18	1.55	0.47
ZS[a]	116	1.0	0.84	16.5	1.485	0.50
G	177	1.0	0.77	21.0	1.466	0.453
A	87	1.244	0.686	28.8	1.45	0.35
B	130	1.244	0.686	35	1.50	0.33

[a] Spin-orbit term with $V_s=5$ MeV included.

same as in the target nucleus. The values extracted from experiment may then be compared to the amplitudes calculated recently by Gillet and Sanderson,[3] for example. The normalization is such that a state which can be described by a unique particle-hole configuration has $g_{lj}=1$ if the hole coincides with that in the target, and zero otherwise.

The single-particle cross section $\sigma_{lj}(\theta)$ was computed using the distorted-wave method. While we shall not describe the general theory, it is necessary to give some preliminary discussion of a few aspects of its application.

2. Optical-Potential Ambiguities

The distorted-wave method does not give a unique prescription for choosing between the various ambiguous potentials which one can obtain from the elastic-scatter-

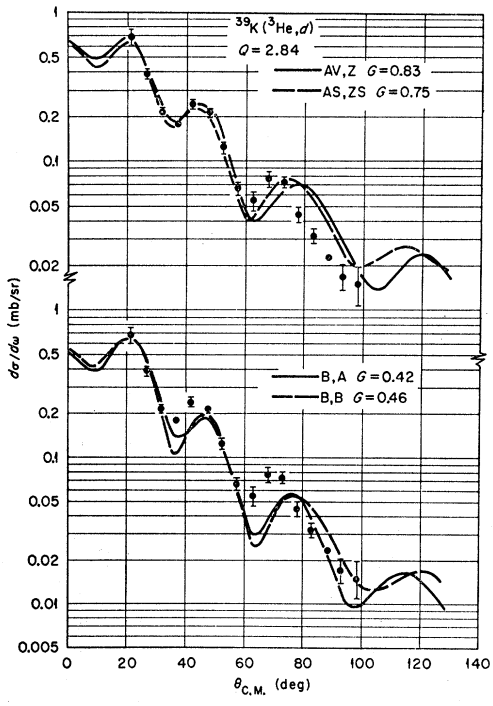

FIG. 8. Comparison with experiment of DW predictions for ^{40}Ca(g.s.). The upper part of the figure shows fits corresponding to the "small radius" ^{3}He and deuteron potentials with and without spin-orbit coupling. The lower part shows the fits corresponding to the "large-radius" potentials. Notice the factor-of-2 change in G_l.

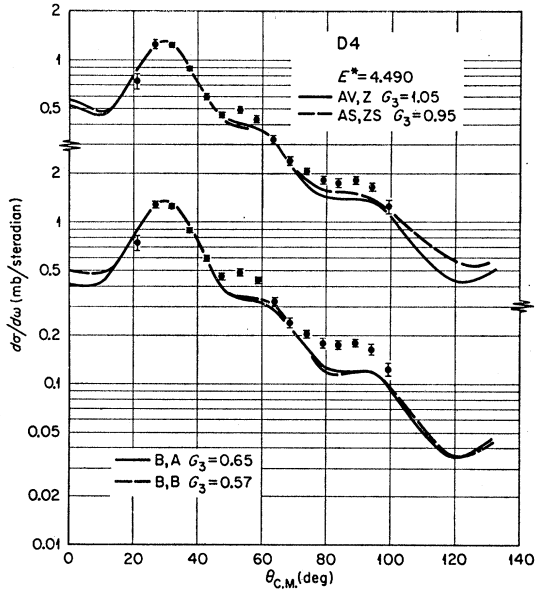

FIG. 9. Comparison with experiment of DW predictions for the 4.490-MeV (5^-) state using both the average potentials with and without spin-orbit coupling (upper part) and the "large-radius" potentials (lower part). Notice again the large change in the spectroscopic factor.

ing data. (Of course, there are no data for scattering from excited states of the residual nucleus, but it is generally assumed one may use the same potentials that describe the scattering from the ground state.) The elastic scattering only determines the form of the wave function outside the nucleus, whereas the reaction is affected by the wave inside the nucleus also. Evidence has been adduced from (d,p) deuteron-stripping reactions that the deuteron potential family with a depth of about 100 MeV gives the most satisfactory agreement when used in a distorted-wave treatment.[22,23] Just as with the ^{3}He scattering discussed above, however, this statement is not unambiguous unless the radius is also specified. Studies of the ^{40}Ca(d,p) reaction[23] showed best results with $V\approx 110$ MeV and $r_0\approx 1.0$ F for the deuterons; shallower potentials gave unacceptable angular distributions, while deeper potentials appeared to yield too large spectroscopic factors for the ground-state transition. For the present work we chose to use the potential of this type (called Z in Table III) which gave a good average fit[24] to the scattering of deuterons of 7 to 12 MeV from ^{40}Ca. It seems consistent to do this in conjunction with the type-A ^{3}He potential, which has a similar radius and a depth about $\frac{3}{2}$ times that for the deuteron. This combination of potentials was used to extract spectroscopic factors from the measurements as described below. However, other choices were tried for the ground state (pure $l=2$, $j=\frac{3}{2}$) and the 4.490-MeV

[22] P. T. Andrews *et al.*, Nucl. Phys. **56**, 465 (1964).
[23] L. L. Lee *et al.*, Phys. Rev. **136**, B971 (1964).
[24] R. H. Bassel *et al.*, Phys. Rev. **136**, B960 (1964).

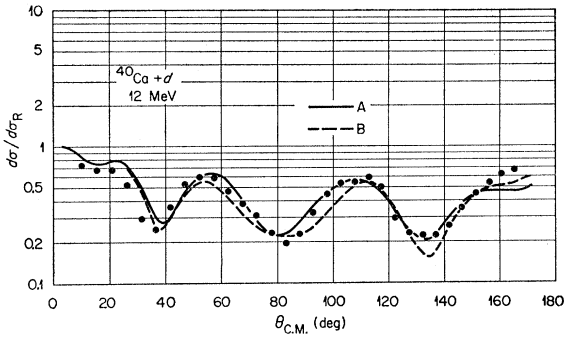

FIG. 10. Optical-model fits to the 12-MeV deuteron elastic-scattering data of Ref. 24, using "large-radius" potentials.

state (pure $l=3$, $j=\frac{7}{2}$), in order to estimate the uncertainties arising in this way.

First, the effect of including spin-orbit coupling in the distorting potentials was studied by using the AS potential of Table II and the ZS potential of Table III. (The latter is an average of the optimum potentials[24] for deuteron scattering from ^{40}Ca at 11 and 12 MeV.) A comparison of the predicted angular distributions with and without spin-orbit coupling for the ground-state transition is shown in the upper part of Fig. 8. The shape changes are small, but perhaps do slightly improve the agreement with experiment. The single-particle cross section $\sigma(\theta)$ predicted at $\theta=20°$ is essentially unchanged, but when the curve is adjusted for an over-all best fit to the data, a reduction of some 10% in the spectroscopic factor results. There is no marked improvement for $\theta>70°$. The upper part of Fig. 9 illustrates the comparable changes for the 5^- state at $E^*=4.490$ MeV.

Next, the ^{3}He potentials of types B and D were used with the type-Z deuteron potential, and also with the next deeper potential G, which fits[24] 11-MeV deuteron scattering from ^{40}Ca. The changes produced were small, but in each case tended to worsen the agreement with the measurements. In particular, the differential cross section tends to fall off more rapidly as one moves away from the peak in the angular distribution.

In view of the prescription which relates the ^{3}He and deuteron potentials to averages of three- and two-nucleon potentials, respectively, it would seem consistent to use the type-B ^{3}He potential in conjunction with a deuteron potential with a similar large radius. The 11-, 11.8-, and 12-MeV deuteron-scattering data were reanalyzed to obtain such a potential with $r_0=1.244$ F and $a=0.686$ F. The prescription would suggest $V\approx100$ MeV; however, as has been found with other nuclei,[25] the data requires either an increase or a decrease of some 20% from this value. Since it is not clear which to use, both were tried. The parameters of the imaginary parts were also optimized; the results are given in Table III and compared to the 12-MeV deuteron-scattering data in Fig. 10.

[25] F. G. Perey and G. R. Satchler, Nucl. Phys. **A97**, 515 (1967).

Again, the distorted-wave predictions for the (^{3}He,d) reactions showed a more rapid decrease with increasing angle when these deuteron potentials A and B were used together with the ^{3}He potential B. Curves for the ground state and the 4.490-MeV state transition are shown in the lower parts of Figs. 8 and 9, respectively; the other transitions exhibit similar characteristics. Although the fall in cross section for the ground state beyond 75° is now reproduced qualitatively, it is only at the expense of a considerable deterioration of fit in the regions of the two subsidiary maxima around 40° and 70°. The magnitudes of the predicted single-particle cross sections are increased by roughly a factor of 2 compared to those from the AV, Z combination of potentials, and the spectroscopic factors are correspondingly reduced. However, part of this increase arises because the proton bound-state wave function used (see below) was computed in a Saxon well of radius $1.25A^{1/3}$ F, whereas the other calculations used $1.20A^{1/3}$ F. This was done in the interests of self-consistency, because the larger radius $r_0=1.244$ for the complex particles was chosen[12,25] partly because of the wide use of $r_0=1.25$ for proton scattering.

While these last results may be taken to indicate that the spectroscopic factors deduced in the present work could be overestimated by as much as a factor of 2, it seems an extreme conclusion because the potentials with large radii give fits to the measured angular distributions which are inferior to those obtained with the AV, Z combination.

3. *Bound-State Wave Function*

The wave function (strictly,[26] form factor) for the captured proton used in the present analysis was taken to be an eigenfunction of motion in a Saxon potential, of radius $r_0A^{1/3}$ and diffuseness a, with a depth adjusted to give a binding energy B equal to the separation energy from the residual state being considered. Thus $B=Q+5.49$ MeV, where Q is the Q value of the transition. For the two highest-excited states observed in the present experiment, this yields negative B values. For these we arbitrarily set $B=0.68$ MeV, the value for the least-tightly-bound state encountered here.

A spin-orbit coupling of strength 25 times the Thomas term was included. It seems likely (and this is supported by the results of structure calculations[3]) that the $l=3$ transitions seen in the present experiment predominantly represent $1f_{7/2}$ capture and that the $l=1$ transitions are $2p_{3/2}$ capture. Hence, all but one transition was computed assuming this. The one exception is the 1^- state at 5.902 MeV; here $l=3$ capture can only be $1f_{5/2}$ while theory[3] suggests roughly equal amounts of $2p_{3/2}$ and $2p_{1/2}$. The calculations were made assuming $1f_{5/2}$ for $l=3$, and with *no* spin-orbit term for the $l=1$. This is not a trivial point. The spin-orbit coupling makes

[26] N. Austern, Phys. Rev. **136**, B1743 (1964); W. T. Pinkston and G. R. Satchler, Nucl. Phys. **72**, 641 (1965).

the wave function for $j=l+\frac{1}{2}$ extend to larger radii, and that for $j=l-\frac{1}{2}$ to contract, compared to a wave function with the same binding in the same well but no spin-orbit coupling.[23] With the spin-orbit strength used here, the cross section for $1f_{7/2}$ capture is about 1.5 times that for $1f_{5/2}$ capture with the *same binding energy*. This difference in cross section for $j=l\pm\frac{1}{2}$ is roughly proportional to $(2l+1)$. The comparison, of course, is unphysical to the extent that one does not expect these two orbits to have the same binding; we return to this point below.

In all the calculations reported here (except those mentioned in the previous section), the values $r_0=1.20$ F and $a=0.65$ F were used. They were chosen partly to facilitate comparison with the earlier analysis[23] of the ^{40}Ca(d,p) reaction, and had been suggested because of some studies of proton scattering from nuclei in this region. A radius $r_0=1.20$ F is probably close to a lower limit on permissible values for this quantity, so the corresponding single-particle cross sections $\sigma(\theta)$ are close to lower limits in this respect also. For example, an increase to $r_0=1.25$ F results in a uniform increase in $\sigma(\theta)$ by about 15% for $l=1$ and 20% for $l=2$ or 3, irrespective of Q value, when the AV, Z combination of potentials is used.

The single-particle wave functions just described are not the same as those used in nuclear-structure calculations. A trivial observation is that the latter are made generally with harmonic-oscillator functions. The point we wish to stress, however, is that structure calculations with two or more particles employ the *same* single-particle wave functions for each member of a multiplet irrespective of their energy differences. For example, the $1f_{7/2}$ proton may be associated with levels in ^{40}Ca differing in energy by 5 MeV or more.[3] (Indeed, two highest-excited states observed in the present experiment are above the proton emission threshold.) However, it would be quite wrong to use the same $1f_{7/2}$ wave function for all the (^{3}He,d) transitions, since it would have the wrong asymptotic form for most of them and the most important contributions come from the nuclear-surface region and outside. (For example, the $l=3$ transition for $E^*=7.660$ MeV was computed with a $1f_{7/2}$ proton bound by 4 MeV. The resulting cross section was nearly a factor of 3 smaller than that obtained by using a proton bound by the actual separation energy, 0.68 MeV.) The form factors that should be used in the stripping calculations[26] will resemble the single-particle wave function used in the structure studies, but modified to take account of the effects of the interaction of the proton with the hole. These will result, for example, in the form factors having the correct asymptotic form which is determined by the separation energy for each level. Our prescription of using eigenfunctions in Saxon well whose depth is adjusted to give a binding equal to the separation energy does yield the correct asymptotic shape, but almost certainly with the wrong normalization.

Some further considerations of this bound-state problem are given in the Appendix.

4. *Nonlocality and Finite-Range Corrections*

Distorted-wave calculations of stripping are often simplified by making the so-called zero-range approximation. It is possible with available codes to make an exact finite-range computation, but fortunately the effects can usually be incorporated into a zero-range calculation by using the local energy approximation.[27] This modulates the bound-state wave function by the factor

$$\Lambda(r)=1-[U_3(r)-U_d(r)-U_p(r)-B_3]/3(\hbar^2/MR^2),$$

where $U_i(r)$ is the optical potential for particle i, B_3 is the binding energy of ^{3}He$=d+p$, M is an atomic mass unit, and R is the "range" (defined, for example, in Ref. 18, from which we take $R=1.54$ F). This approximation is most valid when the departure of Λ from unity is small, and this is seen to occur when the optical potentials satisfy the condition discussed earlier. Its accuracy was rechecked in the present case by comparison with exact calculations for the ground-state transition and using a number of combinations of potentials.

It is believed that the optical potentials should be nonlocal. The local potentials employed should then be regarded as (energy-dependent) local equivalents to these which give the same scattering. However, it has been demonstrated[28] that the wave functions associated with the nonlocal potential, while identical asymptotically, are reduced in the nuclear interior compared to those obtained with the equivalent local potential. Fortunately, for nonlocal potentials of the type usually assumed, this effect can also be incorporated into a distorted-wave calculation with local potentials by using another local-energy approximation modulating factor for each distorted wave,[29]

$$N_i(r)=[1-(\mu_i\beta_i^2/2\hbar^2)U_i(r)]^{-1/2},$$

where μ_i is the reduced mass of the particle, β_i the nonlocality range, and U_i the equivalent local potential. We used $\beta_d=0.54$ F and $\beta_3=0.3$ F. Similar effects are expected for the proton bound state, but we have much less knowledge as to the correct parameters of the nonlocal potential for bound states. While we believe the local-energy approximation correction to be equally valid in this case,[30] it is not at all clear that the local Saxon well we have employed is the equivalent of the "true" nonlocal well in any self-consistent sense. For

[27] P. J. A. Buttle and L. J. B. Goldfarb, Proc. Phys. Soc. (London) **83**, 701 (1964); F. G. Perey and D. Saxon, Phys. Letters **10**, 107 (1964); G. Bencze and J. Zimanyi, *ibid.* **9**, 246 (1964).

[28] F. G. Perey, in *Proceedings of Conference on Direct Interactions, Padua, 1962* (Gordon and Breach Science Publishers, Inc., New York, 1963); N. Austern, Phys. Rev. **137**, B752 (1965).

[29] F. G. Perey and A. M. Saruis, Nucl. Phys. **70**, 225 (1965); other types of nonlocality have been suggested which cannot be treated so simply [R. E. Schenter, Nucl. Phys. **A94**, 408 (1967)].

[30] F. G. Perey (private communication).

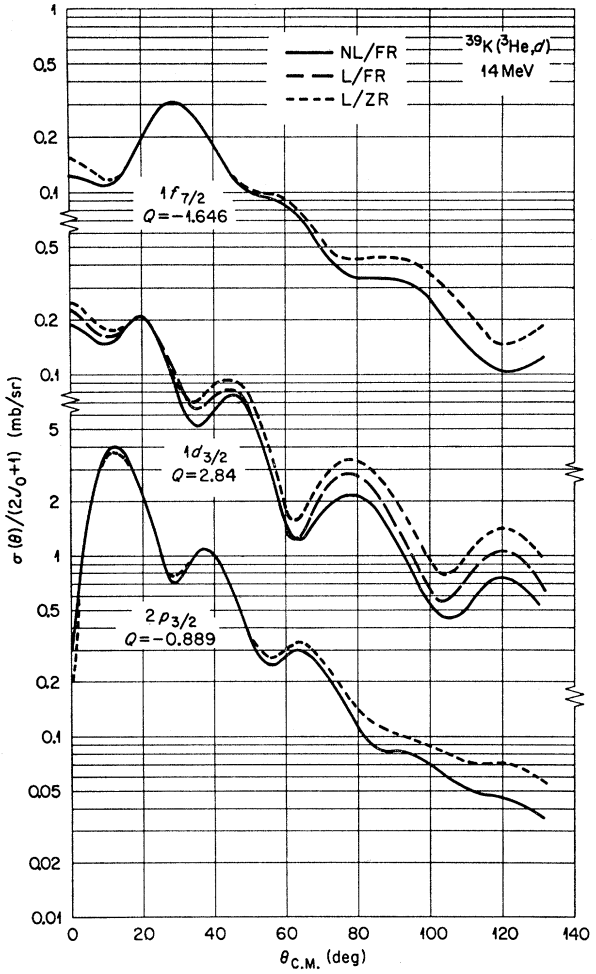

FIG. 11. Illustrating effects of nonlocality and finite range on DW predictions for $l=1$, 2, and 3 transfers.

this reason we have preferred to omit the correction from the computation of the bound-state wave functions. If it had been included, it would have resulted in a reduction of some 30% in the spectroscopic factors deduced. This occurs because the correction factor for bound states has the form $CN_p(r)$, where the constant C is chosen so the corrected wave function is still normalized to unit integral. A typical value of C is 1.15 when $\beta_p=0.85$ F, which enhances the wave-function tail by some 15% and the cross section by some 30%.

The effects of making the zero-range (ZR) approximation compared to the complete finite-range (FR) calculation, and comparisons of using local (L) and nonlocal (NL) distorting potentials, are shown in Fig. 11 for $l=1$, 2, and 3 transitions. The AV, Z combination of optical potentials was used. The effects are rather similar in each case, although most marked for the $1d_{3/2}$ capture. This is because the $1d_{3/2}$ proton is the most strongly bound of the three so the contributions from the nuclear interior are more important. Finite-range and nonlocality effects are also rather similar; in each case the L/FR curves fall roughly midway between the L/ZR and NL/FR curves. The NL/FR *peak* cross sections are slightly larger than those for L/ZR; the ratio is 1.08, 1.05, 1.04 for $l=1$, 2, and 3, respectively.

This, however, may not be a good measure of the differences in spectroscopic factors which would be extracted. The L/ZR cross sections are larger at large angles; if an appreciable weight was given these angles when fitting to the data, we should tend to extract spectroscopic factors which were *smaller* by perhaps 20% than those obtained if the NL/FR curves were used.

5. *Absolute Normalization*

There are two aspects to the absolute normalization of distorted-wave calculations. The first concerns the validity of the approximation itself, the second concerns the numerical value of the normalization constant which appears. The latter includes the overlap of the wave functions for the $d+p$ and ^{3}He systems. We have used the estimate of this given by Bassel[18] [his approximation (b)]; since the cross section predicted is proportional to the square of this number, the corresponding spectroscopic factors deduced from experiment are inversely proportional to its square.

It is difficult to judge how good is the normalization so obtained. Comparisons with experimental data always involve some assumptions about the nuclear structure involved. The most reliable checks perhaps are those concerned with the consistency of data from a range of nuclei.

A comparison with sum-rule predictions for $N=28$ nuclei, for example,[31] yielded agreement to 20%; however, in view of the other uncertainties we have discussed, this could be fortuitous. A study of the ^{48}Ca(^{3}He,d) reaction[18] used potentials similar to those employed here; the NL/FR case would, if nonlocal

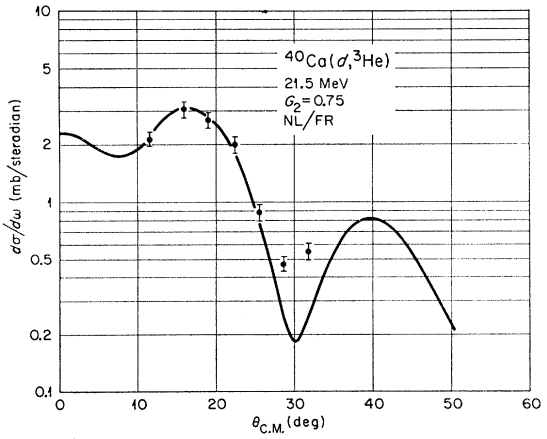

FIG. 12. Comparison with experiment of DW predictions for the 21.5-MeV ^{40}Ca(d,^{3}He)^{39}K(g.s.) data of Ref. 32, using nonlocal potentials and finite range.

[31] D. D. Armstrong and A. G. Blair, Phys. Rev. **140**, B1226 (1965).

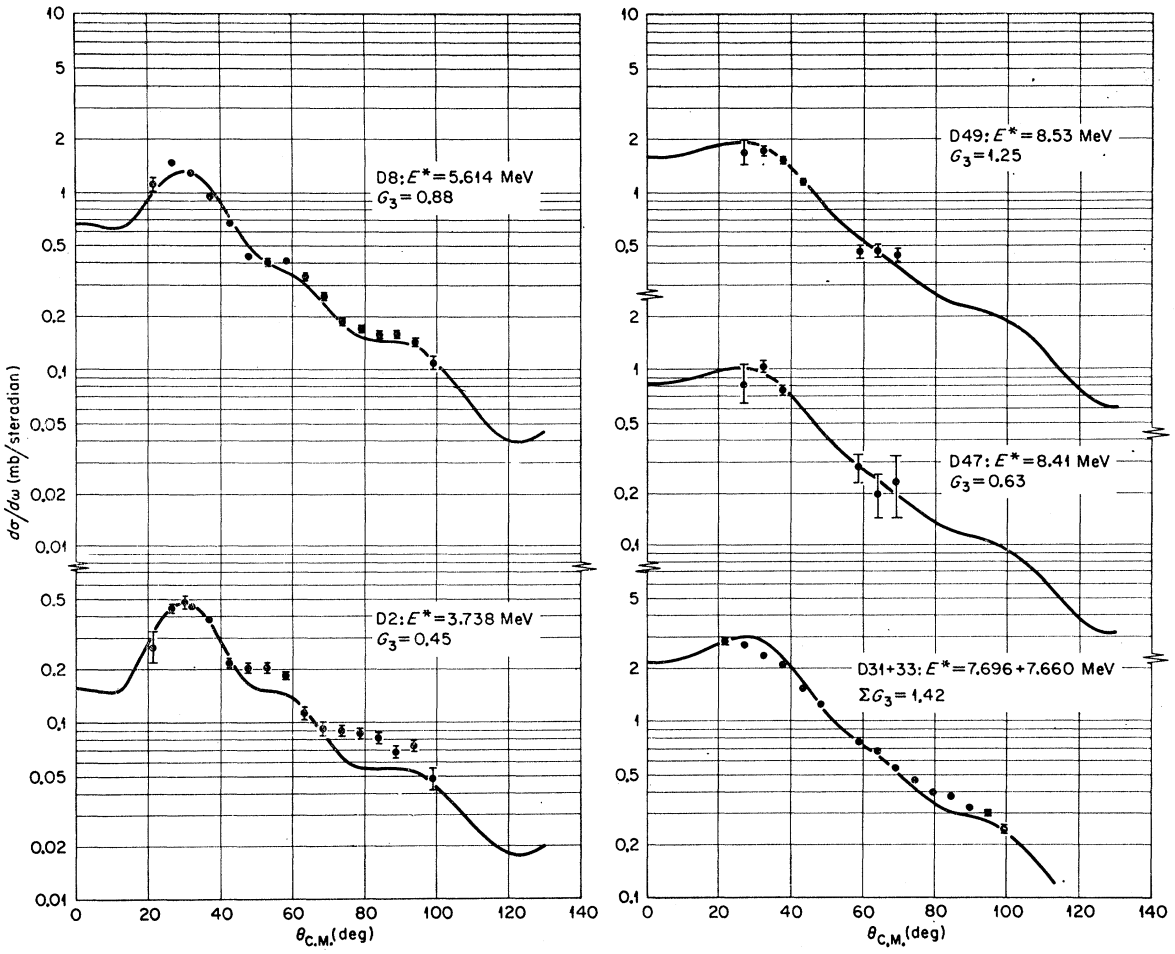

FIG. 13. Comparison with experiment of DW predictions for "pure" $l=3$ transitions.

corrections were omitted from the bound state, give $C^2S\approx 0.86$ for the ground-state transition instead of the value $C^2S=1.0$ expected for a simple closed-shell nucleus. Whether this represents an error of a few percent in the normalization constant, or a fault in the assumptions employed, is not clear. Appealing to the uncertainties in potentials, etc., that we have discussed above, will almost invariably reduce C^2S and increase the apparent discrepancy. On the other hand, correlations in the nuclear wave functions often reduce the expected value of C^2S to below unity, perhaps by an appreciable amount.[3,5] We feel it is reasonable to conclude that the absolute values predicted by the distorted-wave theory used here are certainly correct to better than a factor of 2, and may indeed be much more accurate.

6. $^{40}Ca(d,^3He)$ Reaction

Measurements on this reaction at a deuteron energy of 21.5 MeV have been reported previously.[32] Since the ground-state transition is just the inverse of that studied in the present work (although the energy is about 5 MeV higher), it is of interest to reanalyze that data in the same way so as to obtain a realistic comparison of the spectroscopic factors. This was done, using the same proton bound-state wave function, the AS optical potential of Table II for the ^{3}He, and the deuteron optical potential including spin-orbit coupling which was obtained by Raynal[33] as an optimum fit to the cross sections and polarizations of 22-MeV deuterons scattering from ^{40}Ca. NL and FR corrections were included. The results are compared to the data in Fig. 12. We see that the same strength, $G_2=0.75$, as was found with similar optical potentials for the present experiment (Fig. 8) provides a very good fit to these data also.

The same reaction was studied[14] for a deuteron energy of 34.4 MeV as part of an investigation of the validity of the distorted-wave (DW) method for the $(d,^3\text{He})$ reaction. The same proton wave function was used as here, and NL and FR corrections were included. When the nonlocality corrections to the bound state are

[32] J. L. Yntema and G. R. Satchler, Phys. Rev. **134**, B976 (1964).

[33] J. Raynal, Phys. Letters **7**, 281 (1963).

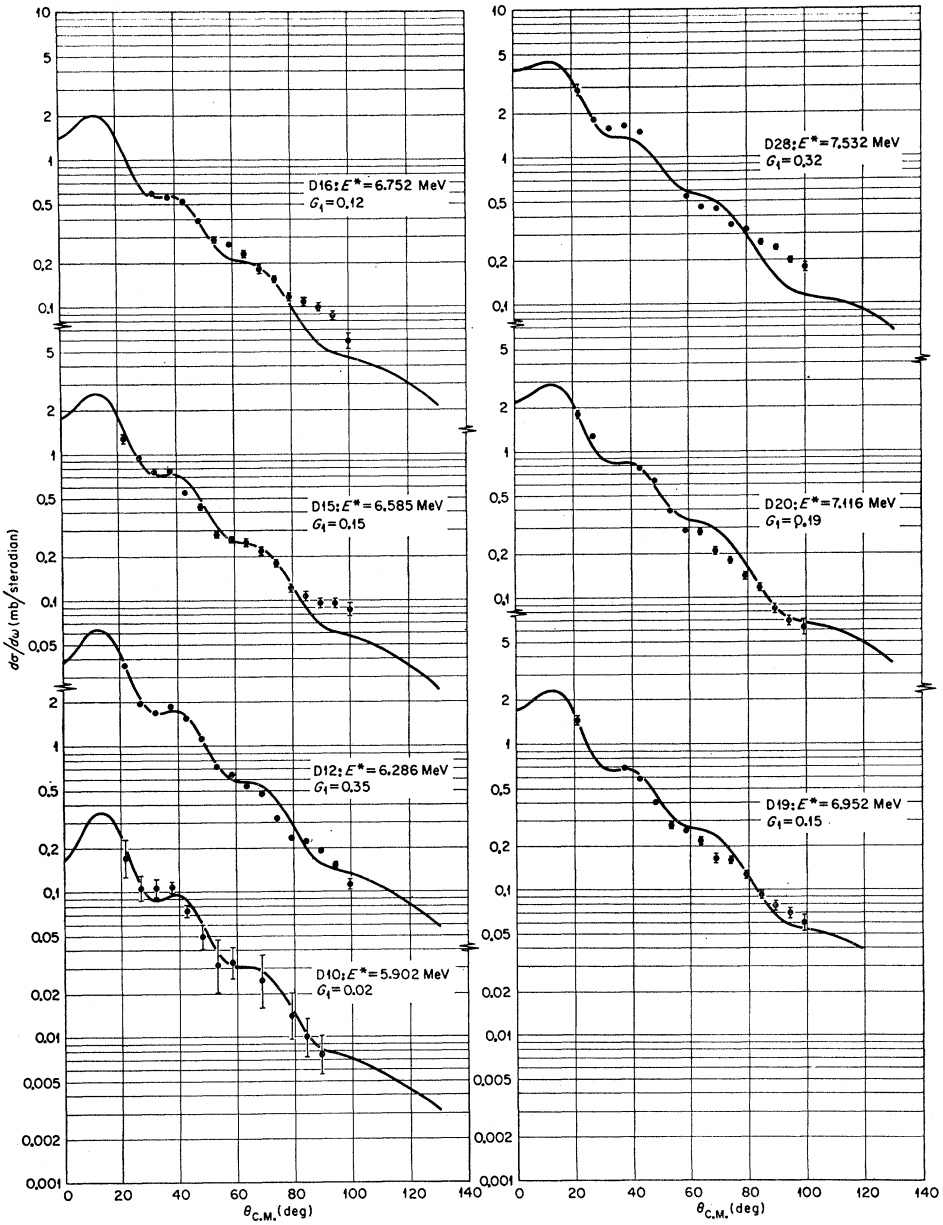

FIG. 14. Comparison with experiment of DW predictions for "pure" $l=1$ transitions.

omitted, as we have done, their analyses give strengths of $G_2 \approx 0.85$ to 1.0, in good agreement with the present work.

V. RESULTS OF DISTORTED-WAVE ANALYSIS

Figures 8, 9, and 13 through 16 show angular distributions for the 16 prominent levels with excitation between 0 and 8.6-MeV observed in this experiment. DW analysis of these angular distributions was done using the nonlocal, finite-range version of the calculations with the average parameters (the potential combination AV, Z) obtained from the analysis of the elastic-scattering data. These are summarized in Table IV.

The analysis of the $l=2$ angular distribution for the ground state of ^{40}Ca and the $l=3$ angular distribution for the 4.490 MeV (5^-) state have already been discussed. All other angular distributions were analyzed for $l=3$ or $l=1$ proton capture into the $1f$ and $2p$ proton orbitals. Some general remarks in this connection are in order. As illustrated in Figs. 11 and 15, the $l=3$ and $l=1$ angular distributions are similar in shape for $\theta \geq 25°$. In case of weak levels this makes l identification and l mixing difficult to determine. The datum at $\theta \simeq 22°$ becomes of crucial importance in these cases.

As is seen in Fig. 15, the predicted $l=3$ single-particle cross sections are approximately a factor of 5 (for $\theta \geq 20°$) to 20 (for $\theta \leq 20°$) smaller than the $l=1$ cross

TABLE IV. Potential parameters used in final DW analysis.

Particle	Type	V (MeV)	r_0 (F)	a (F)	W (MeV)	r_0' (F)	a' (F)	r_c (F)	β (F)
^{3}He	AV	162.0	1.0	0.80	13.0	1.62	0.80	1.40	0.30
d	Z	112.0	1.0	0.90	18	1.55	0.47	1.30	0.54
p[a]		V_p	1.2	0.65	···	···	···	1.25	0

[a] V_p was adjusted to give binding equal to the separation energy from each state; a spin-orbit coupling of 25 times the Thomas term was included.

sections. This means that whereas even small mixtures of $l=1$ can be detected in a predominantly $l=3$ angular distribution by fitting the data for angles less than 25°, even large admixtures of $l=3$ will remain essentially undetected in a strong $l=1$ transition. The agreement between theory and experiment for the ground state and 4.490-MeV levels, for which the l and j values are unique, is a measure of the quality of fit we can obtain. We are probably not justified in assigning much significance to fits better than these which we may obtain by mixing l values. We have, therefore, only made attempts at determining the mixing for two cases of especial interest.

A. Angular Distributions with $l=3$

Figure 13 illustrates pure $l=3$ fits for states at 3.738 (3$^-$), 4.490 (5$^-$), 5.614 (4$^-$), 7.660 (4$^-$)+7.696 (3$^-$), 8.44 (2$^-$), and 8.55 (5$^-$) MeV. While slight improvements here and there may result from the very small amount of $l=1$ mixing that appears permissible, in view of our remarks above it seems meaningless to do this. We can definitely state that, as far as can be determined by the present (DW) analysis of the data, $G_1 \leq 0.02$ for all these states. The values of the strengths G_3 used in drawing the curves in Fig. 13 are given in Table V and in the figure.

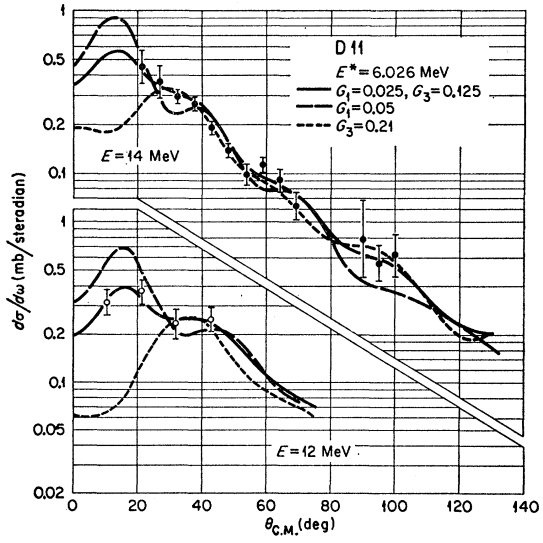

FIG. 15. Comparison of DW predictions with the present data and that of Erskine for the 6.026-MeV level. A mixture of $l=1$ and $l=3$ gives a somewhat better fit.

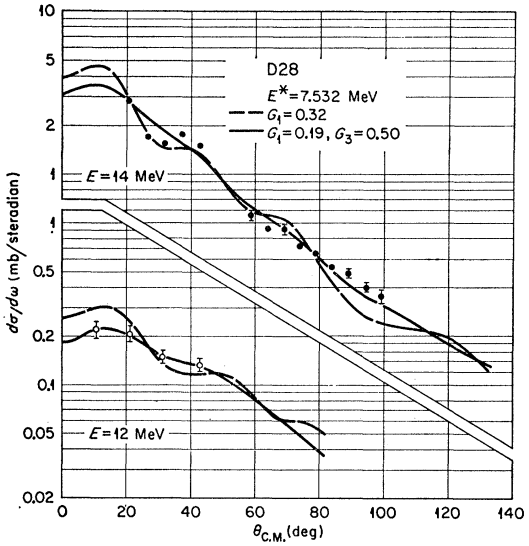

FIG. 16. Comparison of DW predictions with the present data and that of Erskine for the 7.532-MeV level, showing the possibility of having an $l=1+3$ mixture.

B. Angular Distributions with $l=1$

Figure 14 illustrated pure $l=1$ fits for states at 5.902 (1$^-$), 6.286 (3$^-$), 6.585 (3$^-$), 6.752 (3$^-$), 6.952 (1$^-$), 7.116 (3$^-$), and 7.532 MeV. As mentioned above, because of the small cross section predicted for $l=3$, these levels may hide significant amounts of $1f$ strength without changing much the value of S_1 or the quality of fit. A particular example of this, the 7.532-MeV level, is discussed further below. The values of G_1 used in drawing the curves in Fig. 14 are given in Table V and in the figure.

TABLE V. Summary of results from present experiment. The values of G_l or S_l given in parentheses are possible, but not preferred, values. The J values in parentheses were assumed according to the discussion in the text.

Dn	E^* (MeV)	G_1	G_3	J^π	S_1	S_3
$D0$	0	$G_2=0.83$		0$^+$	$S_2=6.64$	
$D2$	3.738	$\lesssim$0.01	0.45	3$^-$	$\lesssim$0.01	0.51
$D4$	4.490	0	1.05	5$^-$	0	0.76
$D8$	5.614	0	0.88	4$^-$	0	0.78
$D10$	5.902	0.02	0	1$^{(-)}$	0.05	0
$D11$	6.026	(0)	(0.21)	(2)$^-$	(0)	(0.34)
		0.025	0.125		0.04	0.20
		(0.05)	(0)		(0.08)	(0)
$D12$	6.286	0.35	0	3$^-$	0.40	$\lesssim$0.1
$D15$	6.585	0.15	0	3$^-$	0.17	0
$D16$	6.752	0.12	0	(0)$^-$	0.96	0
$D19$	6.952	0.15	0	(1)$^-$	0.40	0
$D20$	7.116	0.19	0	(3)$^-$	0.22	0
$D28$	7.532	(0.32)	(0)	(2)$^-$	(0.51)	(0)
		0.19	0.50		0.30	0.80
$D31$	7.660	0	1.42{0.69[a]	4$^-$	0	0.61
$D33$	7.696	0	0.73[a]	3$^-$	0	0.83
$D47$	8.435	0	0.63	2$^-$	0	1.00
$D49$	8.553	0	1.25	5$^-$	0	0.91

[a] Divided in the ratio observed by Erskine (Ref. 6).

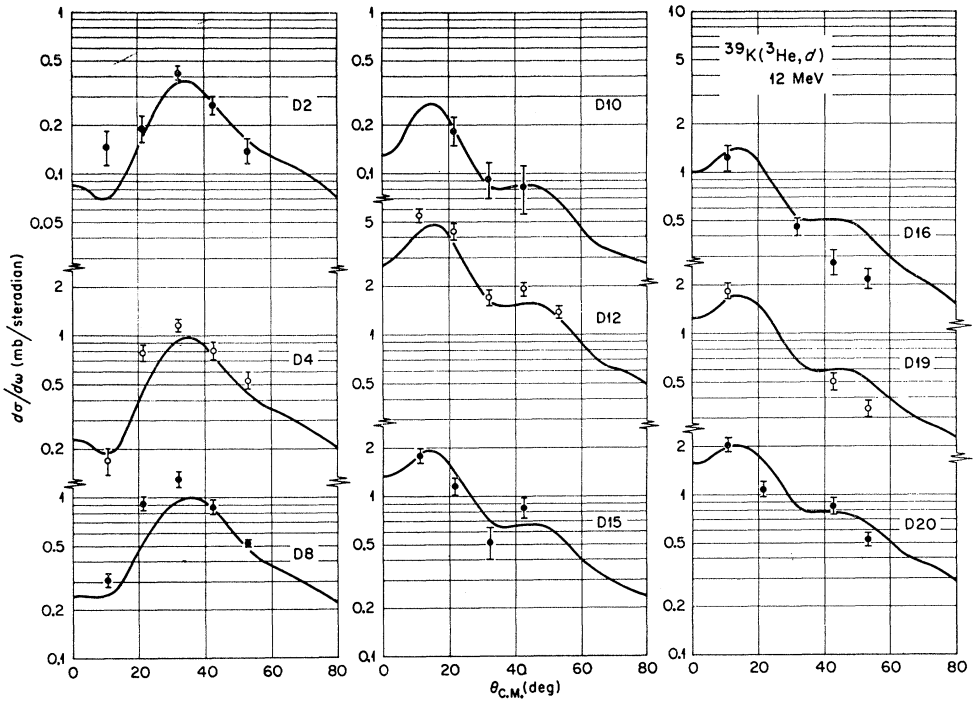

FIG. 17. Comparison of the data taken by Erskine at 12 MeV with DW predictions, using the same parameters as at 14 MeV and strengths G_l deduced from the 14-MeV data (Table VI).

C. Angular Distributions with $l=1$ and $l=3$ Mixed

The transition to the state of 6.026 MeV provides clear evidence for l mixing, which is reinforced by the data of Erskine. This is shown in Fig. 15. The present data are almost consistent with pure $l=1$ ($G_1\approx 0.05$) or, except for $\theta=22°$, with pure $l=3$ ($G_3\approx 0.21$), but the improvement obtained by mixing the two is obvious. The improvement at 12 MeV, where a datum at $\theta\approx 11°$ is available, is not so marked. The mixture used in drawing the curves in Fig. 15 is probably close to the optimum for these data.

For reasons to be discussed below, a similar mixing was tried for the transition to the 7.532-MeV level. The present data are reasonably well described (except at large angles) by pure $l=1$ with $G_1\approx 0.32$. However, as shown in Fig. 16, the fit for large angles is improved and that for small angles is not greatly worsened by having nearly half the cross section due to $l=3$ capture ($G_1\approx 0.2$, $G_3\approx 0.5$). The fit to Erskine's 12-MeV data is almost perfect with this combination, which is therefore preferred over the pure $l=1$ assumption.

D. Comparison with 12-MeV Data

The 12-MeV data of Erskine for two levels have already been mentioned and are included in Figs. 15 and 16. The remaining groups are shown in Fig. 17. A meaningful comparison with our present 14-MeV results requires some estimates of the changes due to the 2-MeV difference in bombarding energies. The simplest way to extrapolate is to use the DW theory together with the optical potentials obtained at 14 MeV. The curves shown in Fig. 17 (as well as those for 12 MeV in Figs. 15 and 16) are DW cross sections obtained with exactly the same parameters as were used to analyze our 14-MeV data, and with the strengths G_l of Table VI deduced from our data. We have already seen that excellent consistency is obtained for the excitation of the 6.026- and 7.532-MeV states. Figure 17 shows there is generally good agreement for the other states also. The 11° cross section for the group $D2$ is somewhat high; this might be taken as evidence for some $l=1$ admixture, but the amount allowed would be severely limited by the 20° cross section; further, the 20° datum at 14 MeV essentially rules out any $l=1$ contribution to this transition. The cross sections for groups $D4$ and $D8$ are higher than expected both at 20° and at 30°, but again an $l=1$ contribution is very unlikely as an explanation, because of both the small 10° cross sections at 12 MeV and the data at 14 MeV. For the $D12$ group one would tend to deduce G_l about 10 to 20% higher from the 12-MeV data than that obtained from our data. On the other hand, for the $D15$ and $D16$ data at 12 MeV alone, one would deduce G_l about 15% lower than ours.

Besides these small differences, Erskine's data is essentially consistent with our results. However, the strengths G_l deduced by Erskine are generally larger than ours, in some cases by as much as a factor of 1.7. Part of this is due to differences in the data and differences in the choice of how to normalize the theoretical

TABLE VI. Spin and parity assignments of states in ^{40}Ca. A lack of entry indicates the level was not observed, or that a spin or parity assignment could not be made. A brace indicates that the various levels in the group embraced were not resolved in that experiment. Spin or parity values in parentheses are tentative.

No.[a]	Excitation energy (MeV)	(e,e')	(α,α')			(p,p')			$(p,p'\gamma)$			$(^3\mathrm{He},d)$		Summary
		120–220 (MeV)[b]	44 (MeV)[c]	51 (MeV)[d]	31 (MeV)[e]	55 (MeV)[f]	17 (MeV)[g]	25 (MeV)[h]	150 (MeV)[i]	13 (MeV)[j]	(MeV)[k]	12 (MeV)[l]	14 (MeV)	
0	0													0^+ [m]
1	3.353													0^+ [m]
2	3.738	3^-		3^-	3^-	3	3		3^-	3^-		3^-	3^-	3^-
3	3.900	2^+		2^+	2^+		2			2^+				2^+
4	4.490	5^-		5^-	5^-	5				5^-		5^-	5^-	5^-
5	5.200			}				}		0, (1)	0^+			0^+
6	5.244			} —				} (1,2)		2	2^+			2^+
7	5.274			}				}		4	4^+			4^+
8	5.614			} —				} $4^{(-)}$		4		4^-	4^-	4^-
9	5.620			}				}			2^+			2^+
10	5.902			3^-	3^-			1^-		1		1^-	1^-	1^-
11	6.026	3^- [n]						$(2^-,4^-)$		3, (2)		(2−)	(2−)	$(2,3)^-$
12	6.286		3^- [p]	3^-	3^-		3	3		3^-		3^-	3^-	3^-
13	6.509													
14	6.544													
15	6.585			3^-	3^-		3	(3)				(3−)	3^-	3^-
16	6.752	3^- [n]							3^-				(0)−	$(2,0)^-$
17	6.91	}	}	} 2^+	(2^+)	}	}	}	(2^+)					2^+
18	6.93	} 2^+ [n]	} 3^- [p]	} or		} $2^+ + 3^-$	} 2	} 1^-						
19	6.952	}	}	} $1^-, 3^-$	$(1^-,3^-)$	}	}	}					1−	1^-
20	7.116						3−						(3)−	
28	7.532												(2)−	
31	7.660											4−	4−	4^-
33	7.696											(3)−	3^-	3^-
46	8.37	} 5^-		} 4^+	} 4^+			} (4,5)						
47	8.44	}		}	}			}				(2−)	2−	2−
48	8.48													
49	8.55	}		} 2^+	} 2^+							(5−)	5−	5^-
50	8.58	}		}	}									

[a] Level sequence is that given by Grace and Poletti (Ref. 10).
[b] Reference 37.
[c] Reference 39.
[d] Reference 34.
[e] Reference 35.
[f] K. Yagi *et al.*, Phys. Letters 10, 186 (1964).
[g] Reference 40.
[h] Reference 38.
[i] Reference 41.
[j] Reference 10.
[k] Reference 36.
[l] Reference 6.
[m] Many experiments, see Ref. 1.
[n] Reported at approximately 0.150 MeV higher energy.
[p] Reported at approximately 0.150 MeV lower energy.

curves to the data. With respect to the latter, our own choices are likely to be preferable because of the larger number of angles available. There are two additional sources of systematic discrepancies. The first arises from the different ^{3}He optical potential used in the DW calculations of Erskine, which results in predicted cross sections some 10% or so smaller than with our potential. His potential was derived from earlier analysis of scattering from ^{40}Ca, rather than from the actual target ^{39}K as was ours. Secondly, we understand that due to an oversight the cross sections shown in Ref. 6 are appropriate to the laboratory coordinate system, but were compared to the center-of-mass DW cross sections. If normalized at 20°, this would lead to an overestimate of the strengths G_l by between 10% (lowest level) and 15% (highest level). Together these two effects would yield strengths which are 20 to 25% larger than our analysis would give.

An exception to the preceding comments is the transition to the 8.44-MeV 2^- state, for which our G_3 is actually 25% larger than Erskine's. Since he states that this group was observed by him only at two angles, his spectroscopic factor is not expected to be very certain.

VI. SPINS AND SPECTROSCOPIC FACTORS

The strengths G_l defined by Eqs. (5) and (6) are given in Table VI. In order to quote values for the spectroscopic factors S_l of Eq. (8) we need to know the spin of the residual nuclear state. In Table VI we summarize the existing information on spin determinations for the states in ^{40}Ca. In the neighborhood of about 7-MeV excitation the level density is so high that uncertainties in energy calibration between different experiments leads to some uncertainties as to which

levels are being observed. There is, for example, a triplet of levels near 6.9 MeV with energies of 6.91, 6.93, and 6.95 MeV which is unresolved in most of the experiments. Beyond 6 MeV the energy calibration of some experiments is also in doubt.

The spins and parities of the ground state and the first ten excited states are known with certainty. The close doublet at 5.614 MeV (4^-) and 5.620 MeV (2^+) has given rise to observations of a group in the (α,α') experiments of Refs. 34 and 35 with characteristics intermediate between those of a 4^- and a 2^+ state. However, the clear-cut identification of these states in the $(p,p'\gamma)$ experiments of Grace and Poletti[10] and MacDonald *et al.*[36] leaves little doubt about the correct assignment of their spins and parities.

The level at 6.026 MeV has been assigned $J=3$ on the basis of the $(p,p'\gamma)$ experiments[10]; a spin 2 is allowed but is only one-fifth as likely. MacDonald *et al.*[36] have looked for γ rays from this state with a high-resolution germanium detector and conclude that should this state be a doublet, the doublet spacing would have to be less than about 10 keV. The (e,e') experiments of Blum *et al.*,[37] do not show either this state or the 6.286-MeV state; instead, a state at 6.16 MeV is reported and $J^\pi=3^-$ assigned to it. As Newton *et al.* have shown, Blum's energies are approximately 0.15 MeV too high for all states in the excitation energy interval 6 to 7 MeV. Their 3^- assignment must refer to the state at 6.286 which has $J^\pi=3^-$ according to all other experiments. The recent (p,p') experiments of Gruhn *et al.*[38] show that the observed angular distribution for the transition to the 6.026-MeV state is consistent with an $l=2$ or 4 angular-momentum transfer and the intensity is small, indicating the possibility that this is a spin-flip transition. While the 3^- assignment cannot be ruled out entirely, we favor the 2^- assignment for this state, as first proposed by Erskine.[6] The inability to observe transitions to this state in all three (α,α') experiments[34,35,39] strengthens our belief in this assignment.

The 3^- assignment for the 6.286- and 6.585-MeV states is certain.

Transitions to the 6.752-MeV state have not been observed in the (α,α') experiments of Refs. 34 and 35 and only weakly observed in the (p,p') experiments of Refs. 10, 38, and 40, indicating that this state is probably a 0^- or 2^-. A strong group corresponding to a state at 6.74±0.07 MeV was reported in the 44-MeV (α,α') experiments of Saudinos *et al.*,[39] who also found a strong group corresponding to a state at 6.16±0.07 MeV. Both these states were assigned $J^\pi=3^-$. These authors did not see the transitions corresponding to the 6.286- and 6.585-MeV states. The (α,α') experiment of Springer *et al.*[34] was done at approximately the same energy with almost twice as good resolution and no trace of these strong groups was seen; instead, strong transitions were seen to the states at 6.28, 6.58, and 6.94 MeV, similar to those observed by Bauer *et al.* at 31 MeV. We contend that Saudinos *et al.* misidentified the so-called 6.16- and 6.74-MeV transitions and that they actually correspond to the states at 6.28 and 6.94 MeV. (The transition corresponding to the 6.58-MeV level is perhaps obscured by the oxygen group in this region.) Rather uncertain evidence for the 6.752-MeV state also comes from the (e,e') experiment of Blum *et al.*,[37] which leads to a 3^- assignment, and the 150-MeV $(p,p'\gamma)$ experiment of Newton *et al.*[41] In the former experiment, the resolution width of nearly 1 MeV makes the level identification difficult. In the latter experiment, a rather weak 6.8-MeV γ ray was the basis of the assignments for both the 6.75- and 6.9-MeV levels. The identification of the observed γ ray to the levels in question as well as the spin assignments are highly debatable. Since this state is strongly excited in our experiment, we deduce that its spin is 0^- or 2^-. From shell-model arguments, to be given later, we prefer the assignment 0^-.

From the accumulated evidence in Table VI, there appears little doubt that of the triplet of levels at 6.91, 6.93, and 6.95 MeV, the 6.95-MeV level is 1^- and at least one of the 6.91- and 6.93-MeV levels is 2^+.

The level at 7.116 MeV has been seen in both the (α,α')[35] and (p,p')[38,40] experiments. In the (α,α') experiment of Bauer *et al.*, the observed transition was weak and poorly resolved from the 6.95-MeV group. Upon careful analysis, the authors have withdrawn their earlier tentative assignment of (6^+). The rather peculiar angular distribution observed probably results from the presence of unresolved transitions to more than one state in this region. Similar remarks apply to the 25-MeV (p,p') experiment of Gruhn *et al.* However, the transition is clearly observed in the (p,p') experiment of Gray *et al.*[40] and it has been unambiguously assigned $l=3$.

TABLE VII. Summed strengths and centroid energies.

Configuration	$\sum G_l$ Observed	$\sum G_l$ Limit	Centroid (MeV) $=\sum(EG_l)/\sum G_l$
$(d_{3/2}^{-1}f_{7/2})$: $T=0$, $l=3$	3.01[a,b]	4	5.28
$(d_{3/2}^{-1}p_{3/2})$: $T=0$, $l=1$	1.20[a]	2	6.77
$(d_{3/2}^{-1}f_{7/2})$: $T=1$, $l=3$	3.30[a]	4	8.16
$(d_{3/2}^{-1}f_{7/2})$: $T=0+1$	6.31[b]	8	6.72

[a] Assumes no T mixing.
[b] Includes the contributions from the assumed 2^- levels.

[34] A. Springer and B. G. Harvey, Phys. Letters **14**, 116 (1965).
[35] R. W. Bauer, A. M. Bernstein, G. Heymann, E. P. Lipincott, and N. S. Wall, Phys. Letters **14**, 129 (1965); E. Lippincott and A. M. Bernstein (to be published).
[36] J. R. MacDonald, D. Start, R. Anderson, and M. A. Grace (private communication, 1967).
[37] D. Blum, P. Barreau, and J. Bellicard, Phys. Letters **4**, 109 (1963).
[38] C. R. Gruhn, T. T. S. Kuo, K. Thompson, and J. Frink, Bull. Am. Phys. Soc. **12**, 585 (1967).
[39] J. Saudinos *et al.*, Compt. Rend. **252**, 260 (1961).
[40] W. S. Gray, R. A. Kenefick, and J. J. Kraushaar, Nucl. Phys. **67**, 542 (1965).
[41] D. Newton, A. B. Clegg, and G. L. Salmon, Nucl. Phys. **67**, 449 (1965).

TABLE VIII. Comparison with calculations of Gillet and Sanderson.

		Particle amplitudes with $d_{3/2}$ hole[a]								Theoretical[b]		Experimental		
	E^*	$f_{7/2}$		$f_{5/2}$		$p_{3/2}$		$p_{1/2}$		S_l		S_l		E^*
J^π	(MeV)	$T=0$	$T=1$	$T=0$	$T=1$	$T=0$	$T=1$	$T=0$	$T=1$	$l=3$	$l=1$	$l=3$	$l=1$	(MeV)
0^-	9.28					−0.85	−0.53				1.90		0.96	6.752
	10.24					−0.53	0.85				0.10			
1^-	3.12[c]			−0.50	−0.01	−0.15	−0.01	−0.25	−0.01					
	8.03			−0.28	−0.01	0.61	0.15	0.52	0.01	0.08	0.86		0.05	5.902
	8.85			−0.25	−0.02	−0.34	−0.20	−0.06	−0.02	0.07	0.30		0.40	6.952
	9.44			0.00	0.01	0.28	0.74	−0.49	−0.21	0.00	1.53			
2^-	7.28	0.95	0.24	0.08	−0.01	0.00	−0.01	0.01	0.00	1.42	0.00	0.80	0.30	7.532
	8.55	0.14	−0.57	0.00	0.05	0.66	0.42	0.12	0.01	0.18	1.18	0.20	0.04	6.026
	8.67	0.19	−0.74	0.01	0.05	−0.56	−0.21	−0.10	−0.02	0.31	0.60	1.00		8.435
	9.61	0.00	−0.09	0.03	0.00	0.43	−0.88	0.14	0.01	0.01	0.23			
	10.96	−0.04	0.00	0.06	−0.02	−0.21	0.06	0.88	0.38	0.00	1.61			
3^-	5.36	−0.62	−0.07	−0.28	0.00	−0.38	−0.03			0.55	0.17	0.51	<0.01	3.738
	7.16	0.59	0.54	−0.03	0.01	−0.45	−0.10			1.28	0.30	<0.1	0.40	6.286
	7.74	0.31	−0.72	0.02	0.02	−0.56	−0.06			0.17	0.38	0.83		7.696
	8.02	−0.36	0.40	0.04	−0.01	−0.47	−0.18			0.00	0.42		0.17	6.585
	9.78	0.02	0.00	−0.02	−0.01	0.19	−0.85			0.00	0.43		0.22	7.116
	10.43	0.07	0.17	−0.11	−0.09	0.01	0.47			0.10	0.23			
	11.66	−0.19	0.04	0.51	0.05	−0.14	0.07			0.33	0.00			
4^-	6.65	0.92	0.39	0.05	0.00					1.72	0.00	0.78		5.614
	7.57	0.39	−0.92	0.02	0.00					0.28	0.00	0.61		7.660
5^-	5.15	0.97	0.11							1.17		0.76		4.490
	8.06	0.10	−0.99							0.79		0.91		8.553

[a] These results are for approximation I (TDA) of Ref. 3.
[b] Calculated assuming that the ^{39}K ground state is a pure $d_{3/2}$ hole.
[c] Spurious state of center-of-mass motion.

The 7.532-MeV transition has not been reported in either the (α,α') or (p,p') experiments. The strong transition to this state observed in Erskine's and our experiments indicates that it is a negative parity state; we tentatively assign it 2^- for reasons based on the shell model.

The remaining four states at 7.660, 7.696, 8.44, and 8.55 MeV seen in the $(^3\text{He},d)$ reaction can be identified as analogs of the known $T=1$ states of ^{40}K and their spins have been assigned by Erskine on that basis. The ground-state analog, expected at 7.622 MeV on the basis of Coulomb displacement energy systematics,[42] has been previously identified at 7.658±0.006 MeV by Rickey *et al.*[43] and 7.646±0.009 MeV by Anderson *et al.*[44] Its observation at the expected energy and the relative spacing of the other three states assures us that the identification of these four states as the analogs of the corresponding states in ^{40}K is correct and that the spin sequence is 4^-, 3^-, 2^-, and 5^-. Strong excitation of these $T=1$ states by inelastic α scattering is not to be expected.

In the last column of Table VI we summarize our conclusions about the J^π of states in ^{40}Ca, and these assignments were used to obtain the spectroscopic factors given in Table V.

[42] D. D. Long, P. Richard, C. F. Moore, and J. D. Fox, Phys. Rev. **149**, 906 (1966).
[43] M. E. Rickey, E. Kashy, and D. Knudsen, Bull. Am. Phys. Soc. **10**, 550 (1965).
[44] W. C. Anderson, L. T. Dillman, and J. J. Kraushaar, Nucl. Phys. **77**, 401 (1966).

VII. DISCUSSION, CONCLUSIONS, AND SPECULATIONS

A. Summary of Experimental Results

Table V summarizes the strengths G_l deduced from the present experiment for the ground and odd-parity excited states of ^{40}Ca, together with the spectroscopic factors S_l which result from the assumed spins and parities J^π. As already mentioned, all the positive-parity excited states were found to be excited extremely weakly. Nevertheless, the 3.351-MeV 0^+ state was seen clearly at $\theta_{\text{lab}}=25°$ to 45°. Its yield was judged to be about 8% of that for the ground state, which gives $G_2\approx 0.06_{-0.03}{}^{+0.01}$ for this transition.

Table VII gives the summed strengths and centroids for the two major odd-parity configurations involved. These numbers were obtained by assuming that the $l=3$ transitions to states below 7.6 MeV of excitation were $f_{7/2}$, and that these states were pure $T=0$. Additional substantial contributions to the $T=0$, $l=3$ strength could be hidden in the groups we have assigned $l=1$, as was explained in Sec. V. In estimating the $p_{3/2}$ strength given in Table VIII it was assumed that all the $l=1$ strength observed was due to this orbital, and again that all the states concerned were pure $T=0$. The recommended mixtures of $l=1+3$ for the $D11$ and $D28$ groups given in Table V were used. The $T=1$, $l=3$ strength quoted comes entirely from the highest quartet of levels in Table V, analogs of the known states in ^{40}K.

B. Ground State

The ground-state strength is 83% of that expected for a simple stripping reaction in which a $d_{3/2}$ hole in a closed shell is filled. This number is obtained within the context of our various choices of optical potentials and proton wave-function parameters. Other choices for the latter might reduce the strength by as much as 30%. Further, we saw (Fig. 8) that it was possible to find optical potentials which would reduce the deduced strength by almost a factor of 2, even though they did give poorer fits to the data. However, any severe reduction in the ground-state strength would also be accompanied by a similar reduction in the other strengths for the excited states and it would begin to be difficult to understand the results as a whole.

It is sometimes said that one should expect a strength considerably less than unity because the ^{40}Ca ground state does not have a good closed-shell character. This does not necessarily follow. It was early shown[45] that the analogous ^{40}Ca(d,p) transition to the ground state of ^{41}Ca could still have a spectroscopic factor of 0.90 even with a 40% core-excitation admixture in the ^{40}Ca ground state, *provided* the ^{41}Ca state contained a similar admixture. The same point has been made again recently by Gerace and Green[5] in connection with the model which mixes spherical and deformed states in ^{40}Ca. Since it is reasonable to suppose that the ground-state correlations in ^{39}K and ^{40}Ca are not very different in structure, they need not destroy the good overlap between the corresponding wave functions and hence can still yield transition strengths close to unity. Supporting evidence for this comes from the very weak excitation of the *excited* 0^+ state. If a large fraction of the $d_{3/2}$ strength had been bled away from the ground-state transition, an appreciable part of it would be expected for excitation of this 0^+ state. These arguments again lend support to the contention that our choice of parameters for the DW analysis was reasonably good and that the ground-state strength is indeed close to unity. If we accept this, the absolute magnitudes of the G_l for the excited states must be taken seriously also.

C. Excited States and the Simple Shell Model

The simplest shell-model picture would predict the centroid energies for the $(j_h^{-1}j_p)$ hole-particle configuration by interpreting the low levels of spin j_p in ^{41}Ca and ^{41}Sc as single-particle states, and those of spin j_h in ^{39}Ca and ^{39}K as single-hole states. This puts the $(d_{3/2}^{-1}f_{7/2})$ configuration at $\sim$7 MeV with $J^\pi=(2,3,4,5)^-$ and both $T=0$ and $T=1$. Experimentally, the centroid is at about 6.7 MeV, with a splitting of about 3 MeV between the centroids of the $T=0$ and $T=1$ quartets. This splitting is in very good agreement with that deduced by French and Bansal[46] (2.8 MeV) and by Zamick[47] (2.9 MeV).

Next, the $(d_{3/2}^{-1}p_{3/2})$, $T=0$, and $T=1$ centroid would be predicted at just over 9 MeV with $J^\pi=(0,1,2,3)^-$, and the $(s_{1/2}^{-1}f_{7/2})$ configuration with $J^\pi=(3,4)^-$ just above. Although the latter configuration would not be directly excited by proton capture, one would expect mixing between these and the states of other configurations. Experimentally, the centroid of that part (60%) observed of the presumed $(d_{3/2}^{-1}p_{3/2})$ $T=0$ strength is at 6.8 MeV.

The centroid of $p_{1/2}$ strength then is expected at just over 11 MeV of excitation, $(d_{3/2}^{-1}p_{1/2})$ with $(1,2)^-$, and close to it and perhaps considerably mixed with it, one would expect the $(s_{1/2}^{-1}p_{3/2})$ with $(1,2)^-$ also. The centroids of the next multiplets would not appear for another 2 MeV or so.

As always, we expect severe mixing in the lowest "collective" 3^- state. Hence, we can expect four strong $l=3$ transitions with possibly some additional $l=3$ from mixing into the next two 3^- states. Also, up to 9 appreciable $l=1$ transitions may be expected, although probably not more than about half these would fall in the range of excitation studied here. Then at 7.7 MeV and above, we expect to see the "$T=1$" levels, analogs of those in ^{40}K. The lowest should be the $(d_{3/2}^{-1}f_{7/2})$ quartet, fed therefore by strong $l=3$ transitions.

How do these simple expectations compare with the observations? The known low-lying 3^-, 5^-, and 4^- have $S_3=0.51$, 0.76, and 0.78, respectively. The reduction from unity for the 4^- and 5^- is similar to that for the ground state, and the additional reduction for the "collective" 3^- is not unexpected. The absence of a good candidate for the 2^- member of this quartet is disturbing. It might be almost degenerate with one of the other states which are excited by $l=1$ capture. The doublet separation could be no more[6,10] than a few keV, and the $l=3$ strength would have to be appreciably less than that for the corresponding $T=1$, 2^- state. None of the transitions is strong enough to conceal all of it without the angular distributions being distorted from the $l=1$ shape. Alternatively, the 6.026-MeV level might be 2^-, as Erskine has suggested. Although assigned $J=3$ from $(p,p'\gamma)$ measurements,[10] the $J=2$ choice is not ruled out. The $l=1+3$ mixture observed could arise from interaction with the nearby $(d_{3/2}^{-1}p_{3/2})$ configuration, resulting in the sharing of the $l=3$ strength.

There are six predominantly $l=1$ transitions observed, in addition to the $l=1$ contributions in the mixed $D11$ and $D28$ groups. The two levels at 6.286 and 6.585 MeV can be identified fairly definitely as 3^-, and probably correspond to the 3^- members of the $(d_{3/2}^{-1}p_{3/2})$ and $(s_{1/2}^{-1}f_{7/2})$ multiplets. The $2p$ spectroscopic factors for these two levels sum to 0.57, so the remaining strength must appear in a higher 3^- state. Six

[45] See the first of Refs. 20, p. 672.

[46] J. B. French and K. Bansal, Phys. Letters **11**, 145 (1966).

[47] L. Zamick, Phys. Letters **19**, 580 (1965).

more 3^-, $T=0$ levels are expected below 20 MeV in the present model, and one could have been pushed down far enough to be the observed 7.116-MeV level for which $J=3$ is possible. If we assume this is 3^-, the spectroscopic factor sum is raised to 0.79, close to the 83% realized for the ground-state $d_{3/2}$ capture.

We also expect a 0^- and 1^- state from the $(d_{2/2}^{-1}p_{3/2})$ configuration in this energy region. The level observed at 5.902 MeV has[10] spin $J=1$ and the present experiment shows odd parity, but its $2p$ spectroscopic factor is only 0.05. However, the various 1^- wave functions may be severely mixed because of the imposed condition that there must be no spurious center-of-mass motion. Another candidate for a $T=0$, 1^- state is the level we excite at 6.952 MeV, as was discussed earlier. If so, it yields $S_1=0.40$. The only possible 0^- level is now that at 6.752 MeV which is not excited by inelastic scattering. The latter is true also of the 7.532-MeV level, but this would give much too large a spectroscopic factor, $S_1\approx 2.5$, if we assumed $J=0$. In addition there is evidence (Fig. 16) of some $l=3$ admixture to this transition which would mean $J\geq 1$. If we assign 0^- to the 6.752-MeV level, we get a spectroscopic factor very close to unity. This could be understood as due to the scarcity of other 0^- states with which it could interact.

Finally, the remaining 2^- level from the $(d_{3/2}^{-1}p_{3/2})$ quartet can be identified with the observed level at 7.532 MeV. We anticipated mixing with the lower 2^- from the $(d_{3/2}^{-1}f_{7/2})$ quartet, and indeed the observed angular distribution in Fig. 16 shows some evidence for $l=1+3$. The choice of $l=3$ strength for the theoretical curve in this figure is an upper limit in the sense that it was made so that together with the 6.026 MeV we obtain unity for the $1f$ spectroscopic factor. However, the largest part of the $l=3$ strength appears in the *upper* of the two states. Further, the $2p$ spectroscopic factors only sum to 0.34; if we had simple mixing between these two configurations alone, the $2p$ factors would also sum to unity. Either our assignments are incorrect or the mixing is more complicated than just between these two configurations alone.

The presumed $T=1$ quartet of the $(d_{3/2}^{-1}f_{7/2})$ configuration, the four states seen above 7.6 MeV, agree very well with theoretical expectations for a pure configuration. Nearly 83% of the expected $l=3$ strength is observed. This is consistent with analysis[20] of the (d,p) reaction feeding the analogous states in ^{40}K. It should be pointed out again, however, that the 8.44- and 8.55-MeV levels in this group are unbound but the DW calculations were made with the binding energy of 0.68 MeV, which is correct for the 7.696-MeV state.

In summary, the observed levels can be assigned spins which are consistent with the levels expected in this energy range on the basis of the simplest shell model with single particle-hole excitations from a closed shell. The $l=3$ strengths are also in reasonable agreement with this picture, but an appreciable part of the $l=1$ strength is missing.

TABLE IX. Values of the quantity $Y_{lj}(R_0)$, defined by Eq. (A3), which is proportional to the reduced width.[a]

Group	B (MeV)	V_p (MeV)	Orbit	$Y_{lj}(R_0)$ ($R_0=5$ F)	$Y_{lj}(R_0)$ ($R_0=6$ F)
$D0$	8.33	58.6	$1d_{3/2}$	0.099	0.0240
$D2$	4.60	62.3	$1f_{7/2}$	0.102	0.0275
		69.1	$2p_{3/2}$	$\lesssim$0.004	$\lesssim$0.0015
$D4$	3.84	61.1	$1f_{7/2}$	0.248	0.0696
$D8$	2.71	59.4	$1f_{7/2}$	0.219	0.0658
$D10$	2.43	66.8	$2p$	0.008	0.0036
$D11$	2.30	58.7	$1f_{7/2}$	0.032	0.0098
		64.9	$2p_{3/2}$	0.010	0.0048
$D12$	2.045	64.4	$2p_{3/2}$	0.141	0.0683
$D15$	1.75	63.8	$2p_{3/2}$	0.061	0.0303
$D16$	1.58	63.5	$2p_{3/2}$	0.049	0.0247
$D19$	1.40	63.1	$2p_{3/2}$	0.062	0.0315
$D20$	1.22	62.8	$2p_{3/2}$	0.078	0.0407
$D28$	0.79	56.4	$1f_{7/2}$	0.135	0.0450
		61.9	$2p_{3/2}$	0.079	0.0428
$D31+32$	0.68	56.2	$1f_{7/2}$	0.392	0.1336
$D47$	0.68	56.2	$1f_{7/2}$	0.174	0.0593
$D49$	0.68	56.2	$1f_{7/2}$	0.345	0.1176

[a] The depth V_p is that required to give a binding energy B with the other parameters given in Table IV.

D. More Sophisticated Models

The simple shell-model considerations of the previous section did not take into account explicitly either the particle-hole residual interactions and the consequent mixing of configurations, or the possibility of the excitation of two or more particles from the closed shell. An early attempt[4] to include the residual interaction used the $SU(3)$ classification for the particle-hole wave functions with L-S coupling, and concluded that these, with $T=S=0$, were a good representation of the low negative-parity states of ^{40}Ca. A central force with a Rosenfeld mixture, adjusted to give the 3^- at 3.73 MeV, predicts the two 1^- levels at about 4.8 and 5.7 MeV, and the two 2^- levels at about 6 and 7 MeV. These are consistent with our assignments within the uncertainties of the model which also predicts, for example, the 4^- excitation to be about 7 MeV instead of the observed 5.6 MeV. A detailed comparison of our deduced spectroscopic factors with the $SU(3)$ wave functions has not been made, but it seems likely that the latter would show more $1f+2p$ mixing than is observed.

Gillet and Sanderson,[3] in a recent revision of their earlier work, have recalculated the odd-parity spectrum of particle-hole states, in two approximations. The relevant parts of the spectrum, and the components of the wave functions which are associated with a $1d_{3/2}$ hole, are given in Table VIII for their approximation I (TDA). Their approximation II (a form of RPA) includes the effects of ground-state correlations. We have not disentangled the parts of these wave functions appropriate to the excited states; however, the changes in the wave functions appear to be small. In order to calculate spectroscopic factors, we need the wave function for the ^{39}K ground state also. The S_l given in Table IX were obtained assuming that it is a simple $d_{3/2}$ hole state. The GS wave functions involve con-

siderable mixing of configurations which are correlated so as to give strong "collective" enhancements of certain transitions, notably that between the ground state and the lowest 3^- state. These have led to good agreement with measurements of the excitation of this 3^- level by the scattering of electrons[48] and of 150-MeV protons.[49] On the other hand, the GS calculations seem to concentrate too much of the octupole strength in this lowest level; the inelastic-scattering measurements[34,35,39] indicate that a large fraction of it remains in the levels at 6.286 and 6.585 MeV, at least.

However, even if agreement with the inelastic transition rates is obtained, this indicates the wave function has the right kinds of correlations with respect to the ground state, but does not necessarily imply that the configurational mixing of the various orbits is correct. The single-nucleon-transfer reaction throws light on a quite different aspect of the wave function, namely its overlap with the ^{39}K ground state. It is not easy to compare the observed spectroscopic factors with those deduced from the GS results because it is often difficult to identify corresponding states. For this reason, the location of some of the experimental results in Table IX is somewhat arbitrary.

The 4^- and 5^- states have a relatively simple structure, being almost entirely $(d_{3/2}^{-1}f_{7/2})$ in agreement with the measurements. However, GS predict strong T mixing, especially for the 4^-, which leads to a greater probability for the lower "$T=0$" states being composed of proton excitation and the higher "$T=1$" states being neutron excitation. The experimental results are consistent with no mixing at all, or possibly even a small mixture in the opposite direction. (The value of S_3 for the 4^- level is based on dividing the $D21+33$ strength between this and the 3^- level in the ratio observed by Erskine, and could be subject to some uncertainty.) In the GS work, the single-particle and single-hole energies used make it slightly easier to excite a proton; perhaps more important is the 0.5-MeV *attractive* Coulomb interaction between the proton particle and hole which was included and which has the same effect.

The identification of the lowest 3^- state is unambiguous, and while the predicted and observed $l=3$ strengths are in good agreement, the predicted $l=1$ strength with $S_1=0.17$ is certainly not present. The 12-MeV data could tolerate $S_1\lesssim 0.01$, while even this amount could not be added at 14 MeV without spoiling the fit to the small-angle data. The next 3^- level, given by GS at 7.16 MeV, is also predicted to be strongly mixed $l=1+3$, whereas the next observed 3^- level at 6.286 MeV is predominantly $l=1$. An $l=3$ strength of perhaps $S_3\lesssim 0.1$ could be present without unduly spoiling the agreement with the 14-MeV data for this group. The large S_3 predicted is due to the constructive T mixing in the wave function.

The next predicted 3^- state (at 7.74 MeV) has $(d_{3/2}^{-1}f_{7/2})$, $T=1$ as its largest component, although because of the severe T mixing, the $l=3$ spectroscopic factor is only $S_3=0.17$. The measurements for the "$T=1$" level at 7.696 MeV are well fitted by a pure $l=3$ transition. Even if the transition were assumed to be pure $l=1$, the $2p$ spectroscopic factor would be only $S_1\approx 0.2$, and the angular distribution shape would be much poorer. It seems reasonable to assume this transition is almost entirely $1f$ capture.

The next two 3^- levels are predicted to be fed by pure $l=1$ capture, and this is consistent with the measurements for the two remaining 3^- states observed. Here however, the observed strengths are only a half of those predicted.

The 2^- states which contain the largest amounts of the $T=0$ and $T=1$ components of the $(d_{3/2}^{-1}f_{7/2})$ configuration are calculated to be at 7.28 and 8.67 MeV, respectively. There is strong T mixing between the theoretical states, and also between them and the $(d_{3/2}^{-1}p_{3/2})$ 2^- states. The $T=0$ member of the latter pair appears most strongly in the state predicted for 8.55 MeV. Again these predictions do not seem to correspond with the measurements. The 2^-, "$T=1$" assignment to the observed 8.41-MeV level seem unambiguous, and the data for this level are consistent with a pure $l=3$ capture. Unfortunately, the shape of the measured angular distribution is not very well determined. A somewhat poorer fit would be obtained with pure $l=1$ and $S_1\approx 0.2$, but even this is much below the predicted $S_1=0.6$.

It was argued earlier that the levels at 6.026 and 7.532 MeV were reasonable candidates for the two remaining 2^- assignments, and $l=1+3$ mixtures were deduced from the transitions to these levels. Neither shows a strong $l=1$ contribution, though the fits shown (Figs. 15 and 16) exhaust the $1f_{7/2}$ capture strength. Even if both transitions were taken to be pure $l=1$, only one-half of the expected $2p$ capture strength would appear and all the $l=3$ strength would have to be found elsewhere. Reasonable fits, close to those shown, put most of the $l=3$ strength into the level with higher energy, contrary to the GS predictions.

We expect two 1^- levels, and these are presumed to be those observed at 5.902 and 6.952 MeV. Both are fed by predominantly $l=1$ transitions, but the lower energy state is much weaker than predicted by GS; $S_1=0.05$ instead of 0.86. The second one is in reasonable agreement with the GS calculations.

Finally, the 0^- state from the $(d_{3/2}^{-1}p_{3/2})$ configuration was identified with the 6.752-MeV level. GS again predict severe T mixing for the 0^- doublet, so much so that the lower member is comprised almost entirely of proton excitation and the upper of neutron excitation. The spectroscopic factor deduced from our identification is almost unity and thus disagrees with GS by a factor of 2. This is in line with our other evidence against T mixing. On the other hand, our value $S_1=0.96$ is in agreement

[48] V. Gillet and M. A. Melkanoff, Phys. Rev. **133**, B1190 (1964).
[49] R. M. Haybron and H. McManus, Phys. Rev. **140**, B638 (1965).

with the GS prediction that there is little *configuration* mixing in the lower 0^- state.

E. Sum Rules

If we make 2^- assignments to the 6.026- and 7.532-MeV levels, and assume the $l=1+3$ mixtures shown in Figs. 15 and 16 and given in Table V, we account for 75% of the $T=0$, $1f_{7/2}$ capture strength expected if the ^{39}K ground state were a simple $d_{3/2}$ hole configuration. This figure of 75% is not out of line with the 83% value found for the ground state. The 2^- states contribute about 0.63 to the sum, so that if these levels were fed only by $l=1$ capture, the $l=3$ strength observed would be reduced to 60% of the sum rule limit for $T=0$. On the other hand, if the 2^- identifications were wrong, but we still allowed the same $l=1+3$ mixture, we would account for 87% of the sum expected (which is 3.475) exclusive of the 2^- contribution. However, in this latter case we would have to postulate that most of the remaining $1f_{7/2}$ capture strength is to be found in 2^- levels at energies higher than those observed here. Alternatively, we could suggest that the ground-state correlations in ^{39}K were such as to block preferentially transitions to the $T=0$, 2^- states, although *a priori* this seems unlikely.

The upper four states which are identified as the $T=1$ quartet from $(d_{3/2}^{-1}f_{7/2})$ indeed exhaust 83% of the sum rule limit for $T=1$, the same percentage of the sum rule as found for the ground-state strength. Since the $T=1$, 2^- identification for the 8.44-MeV level seems reasonably certain, one would certainly expect to find most of the $T=0$, 2^- strength at lower energies. This lends support to our tentative identifications of the lower levels.

Only 60% of the sum-rule limit for the $T=0$, $2p_{3/2}$ strength is accounted for. Even if the 6.026- and 7.532-MeV levels were fed entirely by $l=1$ transitions, this figure would only be increased to 68%. With the spins we have assumed, we find 79% of the expected strength for the 3^- levels, 96% for the 0^- level, but only 45% for the 1^- and 34% for the 2^- levels. Since two more 1^-, 2^- doublets could be expected just above the energy region studied here, the missing strength may be due to configuration mixing with these.

Table VII indicates that 10% more $1f_{7/2}$ capture strength is observed for the upper "$T=1$" levels than for the "$T=0$" levels. If we are not observing some of the $T=1$ strength because of mixing into higher energy states, this excess becomes even larger. At the least, we can say that within the uncertainties of the DW analysis the numbers quoted are consistent with equal strengths for the "$T=0$" and "$T=1$" groups of transitions, which would be the case if there was negligible T mixing and these T values were indeed good quantum numbers. This contrasts strongly with the results of the GS calculations. If we select from Table IX the two GS states for each spin with the largest $T=0$ or $T=1$ $(d_{3/2}^{-1}f_{7/2})$ components, we get a total $l=3$ strength of $G_3=6.7$, or 84% of the limit. However, of this the GS wave functions distribute 62% into the members of the pairs with lower energies, which we may call the "$T=0$" quartet, and only 22% into the upper, so-called "$T=1$," quartet. That is, a ratio of close to three is predicted instead of the near equality observed.

The summed values of the transition strengths G_l tell us about the target nucleus rather than the residual nucleus. For example, the sum-rule limit of 8 said to be "expected" for $1f_{7/2}$ captures is predicated on the $1f_{7/2}$ shell being empty of protons in the ^{39}K ground state. According to Ref. 20, the summed strengths for proton capture are

$$\sum G_l(T=0)=\langle\text{proton holes}\rangle-\tfrac{1}{2}\langle\text{neutron holes}\rangle,$$

$$\sum G_l(T=1)=\tfrac{1}{2}\langle\text{neutron holes}\rangle,$$

where "holes" refers to vacancies in the $1f_{7/2}$ shell in the target nucleus. The naive shell model predicts eight holes each for protons and neutrons (completely empty). The presence of core excitations or ground-state correlations, for example of the 2-particle–3-hole type[5] such as $(d_{3/2}^{-3}f_{7/2}^{2})$, would reduce the sum over G_3 to below the value of 8 by a corresponding amount. By the same token, however, such excitations, if matched closely by the correlations in the ^{40}Ca ground state, could actually increase above unity the $1d_{3/2}$ capture strength G_2 to that state. On the other hand, excitations of the form $(s_{1/2}^{-2}d_{3/2}^{-1}p_{3/2}^{2})$ combined with an equal amount of the corresponding excitation $(s_{1/2}^{-2}p_{3/2}^{2})$ in the ^{40}Ca states would have no effect on the ground-state $d_{3/2}$ capture or the excited $f_{7/2}$ captures but would reduce the $p_{3/2}$ strength. Although our present results are consistent with very little excitation in the ground states of either ^{39}K or ^{40}Ca, clearly even more detailed data and analysis are required before definite conclusions can be drawn.

ACKNOWLEDGMENTS

The authors wish to thank ORTEC for the loan of the experimental Li-drift detector and the prototype particle identifier. We are indebted to R. M. Drisko for making available the optical model code HUNTER and the distorted wave code JULIE, and to R. H. Bassel for helpful discussions concerning the interpretation of the scattering and reaction data. We are also thankful to Richard Couch and Samuel Tabor for considerable help with data analysis.

One of us (K.K.S.) would also like to thank Oak Ridge Associated Universities for their support.

APPENDIX

Some of the uncertainties in the proton wave function to be used in the DW calculations have been discussed. An additional feature, not noted earlier, is that the single-particle potential is isospin-dependent. This was

taken into account in the more sophisticated calculations of Stock and Tamura[50] and can have appreciable effects. The isospin term in the potential has been assumed to give rise to a simple change in either the depth or the radius of the well. In the present case, the diagonal contribution for a proton bound to a $T_0=\frac{1}{2}$ core corresponds to a deeper well (or larger radius) in the $T=0$ state and a shallower well (or smaller radius) in the $T=1$ state. Simply changing the well depth is equivalent to the prescription used in the present work. Keeping the depth constant and varying the radius has the effect of squeezing the proton wave function into smaller radii in the $T=1$ states, and expanding it in the $T=0$ states. Then the spectroscopic factors deduced for the $T=1$ transitions would be *increased* relative to those for the $T=0$ transitions, hence making the discrepancy between the GS predictions and observation even more marked. There are additional effects on the wave functions due to the coupling to the neutron states which is implied, but preliminary calculations[51] indicate that these do not change our conclusions.

Although contributions from the nuclear interior are by no means negligible, the stripping cross sections are found to be almost proportional to the square of the proton wave function $u(r)$ in the exterior region, other things being equal. (This would be strictly true under "Coulomb-stripping" conditions in which the energy would be sufficiently low that the interior contributions would be entirely negligible.) In the exterior region, the correct stripping "form factor"[26] and the proton wave function $u(r)$ used here have the same *form*, hence the observed cross sections give a direct measure of the square of this form factor.

The stripping form factor $R_{lj}(r)$ is defined[26] by the overlap

$$(\psi_{40},\psi_{39})=\sum_{ljT}\langle J_0 j M_0 m|JM\rangle C(T) R_{lj}{}^T(r) Y_{ljm}{}^T, \quad \text{(A1)}$$

where ψ_{40} and ψ_{39} are the wave functions for ^{40}Ca and ^{39}K, respectively, the integral is carried over the coordinates of all the nucleons except the extra one, and $Y_{ljm}{}^T$ is a spin, isospin, and orbital-angular-momentum spinor harmonic for this extra nucleon. In the DW calculations we use a model for the form factor which has the correct tail, namely

$$R_{lj\mathrm{T}}(r)\approx \mathcal{g}_{lj}(T) u_{lj}(r), \quad \text{(A2)}$$

with $u_{lj}(r)$ being the normalized wave function for a proton moving in a Saxon well with a binding equal to the actual separation energy. (The more sophisticated calculations of Stock and Tamura[50] just mentioned included a dependence of $u(r)$ on T also, but that was not done here.) Uncertainty in the optimum choice of parameters for generating $u(r)$ leads to uncertainty in the value of $\mathcal{g}$. It may be useful to partially circumvent these difficulties by returning to the reduced width concept, or something like it. Ignoring isospin mixtures for the moment, the dimensionless reduced width has been defined[20,52] as

$$\theta^2(lj)=S_{lj}\theta_0{}^2(lj),$$

where

$$\theta_0{}^2(lj)=\tfrac{1}{3}R_0{}^3 u_{lj}(R_0)^2$$

is the single-particle reduced width (in units of the Wigner limit value of $3\hbar^2/2MR_0{}^2$) defined in terms of the value of $u_{lj}(r)$ at some radius $r=R_0$. Hence the present analysis could be regarded as giving a measure of θ^2 (rather than of S itself) which would be largely independent of the uncertainties in the choice of the function $u_{lj}(r)$. As examples, we also quote values for the quantity

$$Y_{lj}(R_0)=\tfrac{1}{3}R_0{}^3 u_{lj}(R_0)^2 G_{lj}, \quad \text{(A3)}$$

which

$$=[(2J+1)/(2J_0+1)]C^2\theta^2(lj)$$

in the absence of the isospin mixtures. Of course, θ^2 still depends upon R_0, and the choice of this radius is not unambiguous. The $u_{lj}(r)$ used here do not become asymptotic until $r\gtrsim 7$ F; however, they have turning points mostly between $r\approx 5$ and 6 F. Values of Y_{lj} are given in Table IX for both these radii using the values of G_{lj} from Table V. For example when $R_0=5$ F, $R_0/A^{1/3}=1.46$ F.

[50] R. Stock and T. Tamura, Phys. Letters **22**, 304 (1966), and to be published.

[51] T. Tamura (private communication).

[52] J. B. French, in *Nuclear Spectroscopy*, edited by F. Ajzenberg-Selove (Academic Press Inc., New York, 1960), Part B.